Electronic Supplementary Material (ESI) for ChemComm.

Electronic Supporting Information

One Pot Synthesis and Self-Assembly of Methylene Blue-Backboned Polymers

Xuetong Cai, Luyang Ji, Hao Tang, Rong Wang* and Fude Feng*

Department of Polymer Science & Engineering, School of Chemistry & Chemical Engineering, Nanjing University, Nanjing 210023, P. R. China

*Email: fengfd@nju.edu.cn, wangrong@nju.edu.cn

General methods and materials

The general chemicals and solvents used in this work were commercially available and were used as received without further purification unless stated otherwise.

NMR spectra were recorded on a Bruker AMX 400 spectrophotometer with use of residual solvent or TMS as the internal reference. Fourier transform infrared (FT-IR) spectra were collected on a ThermoFisher Nicolet iS50 FT-IR spectrometer. Ultraviolet-visible (UV/Vis) absorption spectra were measured on a Shimadzu UV–2600 spectrophotometer. Fluorescence spectra were taken on a Hitachi F–7000 fluorimeter. Transmission electron microscopy (TEM) images were collected on JEM–1011 (JEOL, Ltd., Japan). Atomic force microscopy (AFM) images were taken on a Bruker Dimension ICON mass spectrometer (Bruker, USA). Gel permeation chromatography (GPC) measurements were performed on a Waters 515 (America) using DMF as an eluting agent at a flow rate of 1.0 mL min^{-1} at 35 °C and with a Waters 244 equipped with an internal refractive index (RI) detector and a PL1110–6504 column, calibrated in relation to polyethylene glycol standards.

Experimental section

Synthesis of 1a-d

General procedure: A mixture of the appropriate diamine (3.5 mmol), potassium carbonate (2.9 g, 21 mmol) and *p*-fluoronitrobenzene (1.06 g, 7.5 mmol) in DMF (35 mL) was stirred overnight at 130−160 °C, and cooled to the room temperature. Deionized water (100 mL) was added and the mixture was filtered. The yellow residue was washed with deionized water and subsequent isopropyl alcohol/isopropyl ether (1:1, v/v), and recrystallized in DMSO.

1a: 1,4-Butanediamine (0.31 g, 3.5 mmol) was reacted at 130 °C to afford **1a** (0.98 g, 85 %) as a yellow solid. ^{1}H NMR (400 MHz, DMSO–6d): δ 7.99 (d, *J* = 9.3 Hz, 4H), 7.31–7.33 (t, *J* = 5.3 Hz, 2H), 6.65 (d, *J* = 9.4 Hz, 4H), 3.19 (d, *J* = 5.5 Hz, 4H), 1.65–1.68 (m, 4H) ppm. ^{13}C NMR (101 MHz, DMSO–6d), δ 154.55, 135.44, 126.24, 110.69, 41.98, 25.81 ppm. MS, calculated for $[M+H]^+$: 331.14, found $[M+H]^+$: 331.00.

1b: 1,6-Hexanediamine (0.41 g, 3.5 mmol) was reacted at 130 °C to afford **1b** (1.14 g, 91%) as a yellow solid. ^{1}H NMR (400 MHz, DMSO–6d): δ 7.98 (d, J = 9.3 Hz, 4H), 7.29 (t, J = 5.3 Hz, 2H), 6.62 (d, J = 9.4 Hz, 4H), 3.14 (dd, J = 12.6, 6.8 Hz, 4H), 1.67 – 1.49 (m, 4H), 1.40 (t, J = 6.9 Hz, 4H) ppm. ^{13}C NMR (101 MHz, DMSO–6d), δ 154.56, 135.38, 126.23, 110.59, 42.26, 28.23, 26.22 ppm. MS, calculated for $[M+H]^+$:

359.17, found $[M+H]^+$: 359.05.

1c: 1,8-Octanediamine (0.51 g, 3.5 mmol) was reacted at 140 °C to afford **1c** (1.19 g, 88%) as a yellow solid. ^{1}H NMR (400 MHz, DMSO–6d): δ 7.98 (d, J = 9.3 Hz, 4H), 7.28 (t, J = 5.3 Hz, 2H), 6.62 (d, J = 9.4 Hz, 4H), 3.12 (dt, J = 11.7, 5.9 Hz, 4H), 1.55 (dd, J = 13.9, 7.0 Hz, 4H), 1.44 – 1.22 (m, 8H) ppm. ^{13}C NMR (101 MHz, DMSO–6d), δ 154.58, 135.36, 126.23, 110.59, 42.31, 28.72, 28.25, 26.43 ppm. MS, calculated for $[M+H]^+$: 387.20, found $[M+H]^+$: 387.10.

1d: 1,10-Decanediamine (0.61 g, 3.5 mmol) was reacted at 160 °C to afford **1d** (1.26 g, 87%) as a yellow solid. ^{1}H NMR (400 MHz, DMSO–6d): δ 7.98 (d, J = 9.3 Hz, 4H), 7.27 (t, J = 5.6 Hz, 2H), 6.62 (d, J = 9.4 Hz, 4H), 3.12 (dt, J = 10.4, 5.2 Hz, 4H), 1.68 – 1.41 (m, 4H), 1.31 (dd, J = 15.8, 9.7 Hz, 12H) ppm. ^{13}C NMR (101 MHz, DMSO–6d), δ 154.59, 135.35, 126.25, 110.60, 42.31, 28.93, 28.73, 28.26, 26.46 ppm. MS, calculated for $[M+H]^+$: 415.23, found $[M+H]^+$: 415.15.

Synthesis of 2a-2f

General procedure: To a solution of compound **1** (3.3 mmol) in anhydrous DMF (10 mL) cooled to 0 °C, sodium hydride (0.50 g, 20.8 mmol) was added. The mixture was stirred at room temperature for 1 h, and cooled to 0 °C. Appropriate iodoalkane (13.2 mmol) was added dropwise. After stirring for 12 h at 25−60 °C, deionized water (100 mL) was added. The mixture was and stirred for 1 h and filtered. The yellow solid was washed with deionized water and methanol, and dried under reduced pressure.

2a: **1a** (1.09 g, 3.3 mmol) was reacted with ethyl iodide (3.0 g, 13.2 mmol) at room temperature to afford **2a** (1.02 g, 80 %) as a yellow solid. ^{1}H NMR (400 MHz, DMSO–6d): δ 8.02 (d, J = 9.1 Hz, 4H), 6.78 (d, J = 9.3 Hz, 4H), 3.47 (dd, J = 13.4, 6.0 Hz, 8H), 1.62 (s, 4H), 1.13 (t, J = 6.8 Hz, 6H) ppm. ^{13}C NMR (101 MHz, DMSO–6d), δ 152.37, 134.95, 126.09, 110.42, 49.55, 44.65, 24.15, 11.99 ppm. MS, calculated for $[M+H]^+$: 387.20, found $[M+H]^+$: 387.05.

2b: **1b** (1.18 g, 3.3 mmol) was reacted with ethyl iodide (3.0 g, 13.2 mmol) at room temperature to afford **2b** (1.19 g, 87 %) as a yellow solid. ^{1}H NMR (400 MHz, DMSO–6d): δ 8.01 (d, J = 9.4 Hz, 4H), 6.74 (d, J = 9.5 Hz, 4H), 3.48 (q, J = 7.0 Hz, 4H), 3.43 – 3.36 (m, 4H), 1.57 (s, 4H), 1.37 (s, 4H), 1.12 (t, J = 7.0 Hz, 6H) ppm. ^{13}C NMR (101 MHz, DMSO–6d), δ 152.92, 135.45, 126.58, 110.79, 50.21, 45.28, 27.24, 26.51, 12.49 ppm. MS, calculated for $[M+H]^+$: 415.23, found $[M+H]^+$: 415.15.

2c: **1c** (1.27 g, 3.3 mmol) was reacted with ethyl iodide (3.0 g, 13.2 mmol) at room temperature to afford **2c** (1.20 g, 82 %) as a yellow solid. ^{1}H NMR (400 MHz, DMSO–

6d): δ 8.02 (d, J = 9.5 Hz, 4H), 6.73 (d, J = 9.5 Hz, 4H), 3.47 (q, J = 7.0 Hz, 4H), 3.41 – 3.35 (m, 4H), 1.55 (s, 4H), 1.31 (s, 8H), 1.12 (t, J = 7.0 Hz, 6H) ppm. ^{13}C NMR (101 MHz, DMSO–6d), δ 152.93, 135.43, 126.59, 110.78, 50.29, 45.27, 29.31, 27.32, 26.67, 12.47 ppm. MS, calculated for $[M+H]^+$: 443.27, found $[M+H]^+$: 443.15.

2d: **1d** (1.37 g, 3.3 mmol) was reacted with ethyl iodide (3.0 g, 13.2 mmol) at room temperature to afford **2d** (1.24 g, 80 %) as a yellow solid. ^{1}H NMR (400 MHz, DMSO–6d): δ 8.02 (d, J = 9.5 Hz, 4H), 6.73 (d, J = 9.6 Hz, 4H), 3.52 – 3.38 (m, 8H), 1.54 (s, 4H), 1.30 (s, 12H), 1.12 (t, J = 7.0 Hz, 6H) ppm. ^{13}C NMR (101 MHz, DMSO–6d), δ 152.91, 135.44, 126.58, 110.76, 50.30, 45.27, 29.41, 29.30, 27.31, 26.73, 12.47 ppm. MS, calculated for $[M+H]^+$: 471.30, found $[M+H]^+$: 471.20.

2e: **1d** (1.37 g, 3.3 mmol) was reacted with 1-iodobutane (2.43 g, 13.2 mmol) at 50°C to afford **2e** (1.53 g, 88 %) as a yellow solid. ^{1}H NMR (400 MHz, DMSO–6d): δ 8.01 (d, J = 9.5 Hz, 4H), 6.72 (d, J = 9.6 Hz, 4H), 3.42 – 3.36 (m, 8H), 1.53 (d, J = 5.5 Hz, 8H), 1.36 – 1.21 (m, 16H), 0.91 (t, J = 7.3 Hz, 6H) ppm. ^{13}C NMR (101 MHz, DMSO–6d), δ 153.09, 135.42, 126.53, 110.83, 50.82, 50.61, 29.38, 29.27, 27.09, 26.67, 19.98, 14.23 ppm. MS, calculated for $[M+H]^+$: 527.36, found $[M+H]^+$: 527.30.

2f: **1d** (1.37 g, 3.3 mmol) was reacted with 1-bromooctane (2.55 g, 13.2 mmol) at 60°C to afford **2f** (1.77 g, 84 %) as a yellow solid. ^{1}H NMR (400 MHz, DMSO–6d): δ 8.01 (d, J = 9.5 Hz, 4H), 6.71 (d, J = 9.5 Hz, 4H), 3.42 – 3.35 (m, 8H), 1.53 (s, 8H), 1.31 – 1.20 (m, 32H), 0.84 (t, J = 6.8 Hz, 6H) ppm. ^{13}C NMR (101 MHz, DMSO–6d), δ 150.62, 134.94, 126.04, 110.36, 50.34, 31.18, 28.83, 28.76, 28.73, 28.66, 26.63, 26.59, 26.20, 26.14, 22.03, 13.89 ppm. MS, calculated for $[M+H]^+$: 639.48, found $[M+H]^+$: 639.45.

Synthesis of DIAs

General procedure: To a solution of compound **2** (2.8 mmol) in methanol (50 mL) were added acetic acid (3.0 g, 50 mmol) and zinc powder (1.96 g, 30 mmol). The mixture was stirred at 60 °C for 12 h. The aqueous phase was separated and the pH was adjusted to approximately 9 by sodium hydroxide. After extraction with ethyl acetate (3×30 mL), the combined organic phase was washed with deionized water (3×100 mL), dried over anhydrous sodium sulfate, and evaporated to give the final product.

DIA1: **2a** (1.08 g, 2.8 mmol) was reacted to afford DIA1 (0.67 g, 73 %) as a dark yellow viscous liquid. ^{1}H NMR (400 MHz, DMSO–6d): δ 6.50 (dd, J = 23.4, 8.6 Hz, 8H), 4.39 (s, 4H), 3.13 – 2.91 (m, 8H), 1.40 (s, 4H), 0.94 (t, J = 7.0 Hz, 6H) ppm. ^{13}C NMR (101 MHz, DMSO–6d), δ 140.22, 139.66, 116.94, 115.22, 51.13, 45.83, 24.71, 12.22 ppm. MS, calculated for $[M+H]^+$: 327.25, found $[M+H]^+$: 327.10.

DIA2: **2b** (1.16 g, 2.8 mmol) was reacted to afford DIA2 (0.81 g, 82 %) as a dark yellow viscous liquid. ^{1}H NMR (400 MHz, DMSO–6d): δ 6.49 (dd, J = 19.6, 8.7 Hz, 8H), 4.38 (s, 4H), 3.08 (q, J = 6.8 Hz, 4H), 3.04 – 2.90 (m, 4H), 1.38 (s, 4H), 1.25 (s, 4H), 0.94 (t, J = 7.0 Hz, 6H) ppm. ^{13}C NMR (101 MHz, DMSO–6d), δ 140.08, 139.91, 118.70, 115.26, 51.16, 45.80, 27.03, 26.58, 12.22 ppm. MS, calculated for $[M+H]^+$: 355.29, found $[M+H]^+$: 355.20.

DIA3: **2c** (1.24 g, 2.8 mmol) was reacted to afford DIA3 (0.82 g, 77 %) as a dark yellow viscous liquid. ^{1}H NMR (400 MHz, DMSO–6d): δ 6.63 – 6.35 (m, 8H), 4.38 (s, 4H), 3.09 (q, J = 7.0 Hz, 4H), 3.03 – 2.90 (m, 4H), 1.37 (d, J = 6.1 Hz, 4H), 1.24 (s, 8H), 0.94 (t, J = 7.0 Hz, 6H) ppm. ^{13}C NMR (101 MHz, DMSO–6d), δ 140.61, 140.40, 117.24, 115.73, 51.73, 46.29, 29.49, 27.53, 27.12, 12.71 ppm. MS, calculated for $[M+H]^+$: 383.32, found $[M+H]^+$: 383.20.

DIA4: **2d** (1.32 g, 2.8 mmol) was reacted to afford DIA4 (0.86 g, 75 %) as a dark yellow viscous liquid. ^{1}H NMR (400 MHz, DMSO–6d): δ 6.49 (dd, J = 20.9, 8.7 Hz, 8H), 4.39 (s, 4H), 3.09 (q, J = 6.9 Hz, 4H), 3.03 – 2.90 (m, 4H), 1.38 (s, 4H), 1.23 (s, 12H), 0.94 (t, J = 7.0 Hz, 6H) ppm. ^{13}C NMR (101 MHz, DMSO–6d), δ 140.09, 116.74, 115.24, 51.23, 28.96, 27.06, 26.66, 12.23 ppm. MS, calculated for $[M+H]^+$: 411.35, found $[M+H]^+$: 411.25.

DIA5: **2e** (1.47 g, 2.8 mmol) was reacted to afford DIA5 (1.04 g, 80 %) as a dark yellow viscous liquid. ^{1}H NMR (400 MHz, DMSO–6d): δ 6.49 (q, J = 8.8 Hz, 8H), 4.38 (s, 4H), 3.01 (t, J = 6.8 Hz, 8H), 1.44 – 1.30 (m, 8H), 1.31 – 1.17 (m, 16H), 0.87 (t, J = 7.3 Hz, 6H) ppm. ^{13}C NMR (101 MHz, DMSO–6d), δ 140.71, 140.52, 117.08, 115.72, 52.45, 52.18, 29.67, 29.48, 29.41, 27.40, 27.11, 20.32, 14.39 ppm. MS, calculated for $[M+H]^+$:467.41, found $[M+H]^+$: 467.30.

DIA6: **2f** (1.79 g, 2.8 mmol) was reacted to afford DIA6 (1.18 g, 73 %) as a dark yellow viscous liquid. ^{1}H NMR (400 MHz, DMSO–6d): δ 6.47 (d, J = 6.0 Hz, 8H), 4.41 (s, 4H), 2.98 (s, 8H), 1.37 (s, 8H), 1.23 (s, 32H), 0.84 (dd, J = 8.4, 5.2 Hz, 6H) ppm. ^{13}C NMR (101 MHz, DMSO–6d), δ 140.72, 140.54, 117.07, 115.69, 52.47, 31.74, 29.41, 29.23, 27.43, 27.12, 27,10, 22,57, 14.38 ppm. MS, calculated for $[M+H]^+$: 579.54, found $[M+H]^+$: 579.50.

Preparation of MBPs:

General procedure: To a solution of DIA (0.37 mmol) in HCl (2.0 M, 10 mL) were added sodium sulfide hydrate (180 mg, 0.75 mmol) and a solution of ferric chloride hexahydrate (300 mg, 1.11 mmol) in HCl (1.0 M, 10 mL) in sequence. The mixture was stirred for 0.5 h at 37 ° C, and sodium sulfite (300 mg, 2.38 mmol) was added to reduce ferric ions. After stirring for 0.5 h, the pH was adjusted to 3 with sodium hydroxide. The mixture was dialyzed against 0.1 M HCl for 4 days and deionized water for 2 days with a molecular weight cutoff of 3500 Da, and lyophilized to obtain MBP as a dark blue solid.

MBP1: DIA1 (121 mg, 0.37 mmol) was reacted to afford MBP1 (18.1 mg, 15 %). ^{1}H NMR (400 MHz, DMSO–6d): δ 6.91–7.91 (br, 6 H), 3.73 (br, 8 H),0.85–1.59 (br, 10 H).

MBP2: DIA2 (131 mg, 0.37 mmol) was reacted to afford MBP2 (15.7 mg, 12 %). ^{1}H NMR (400 MHz, DMSO–6d): δ 6.89–7.90 (br, 6 H), 3.67 (br, 8 H), 0.86–1.68 (br, 14 H).

MBP3: DIA3 (141 mg, 0.37 mmol) was reacted to afford MBP3 (18.4 mg, 13 %). ^{1}H NMR (400 MHz, DMSO–6d): δ 6.57–7.90 (br, 6 H), 3.73 (br, 8 H), 0.76–1.62 (br, 18 H).

MBP4: DIA4 (151 mg, 0.37 mmol) was reacted to afford MBP4 (18.2 mg, 12 %). ^{1}H NMR (400 MHz, DMSO–6d): δ 6.71–7.90 (br, 6 H), 3.65 (br, 8 H),0.85–1.62 (br, 22 H).

MBP5: DIA5 (172 mg, 0.37 mmol) was reacted to afford MBP5 (29.3 mg, 17 %). ^{1}H NMR (400 MHz, DMSO–6d): δ 6.66–7.90 (br, 6 H), 3.64 (br, 8 H),0.85–1.61 (br, 30 H).

MBP6: DIA6 (214 mg, 0.37 mmol) was reacted to afford MBP6 (30.0 mg, 14 %). ^{1}H NMR (400 MHz, DMSO–6d): δ 7.37–7.91 (br, 6 H), 3.42–3.68 (br, 8 H),0.83–1.63 (br, 46 H).

The ^{1}H NMR spectra of MBPs were shown in Fig. S18-S23. The FT-IR spectra of MBPs were shown in Fig. S25c.

Imaging of MBPs by transmission electron microscopy (TEM)

The polymer solutions were prepared by the co-solvent method. The polymer solutions (5 μL) were dropped onto the 100-mesh copper grids with carbon-coated formvar support. After 20 min, the extra solutions were wicked off using the filter paper. The samples were subjected to TEM imaging without staining. All the images were recorded on JEM–1011 instrument at 100 kV.

Imaging of MBPs by atomic force microscopy (AFM)

The polymer solutions were prepared by the co-solvent method. The polymer solutions (20 μL) were dropped onto the freshly cleaved mica substrate (1 cm×1 cm). After 30 min at room temperature, the extra solution was blown away by a gentle stream of argon, air dried overnight under ambient conditions, and subjected to AFM imaging.

Simulation method and model

The DPD method, introduced by Hoogerbrugge and Koelman [1] in 1992 and improved by Español and Warren [2] in 1995, is a widely used mesoscopic simulation approach.[3] In DPD simulations, an individual particle represents a cluster of atoms or molecules. The use of soft potential and a reduced number of interaction sites makes it a valuable approach to describe the phase morphology and dynamics of numerous soft matter systems at mesoscale while retaining the correct hydrodynamics. The time evolution of the simulation system is governed by integrating Newton's equation of motion:[4]

$$\frac{\mathrm{d}\vec{r}_i}{\mathrm{d}t}=\vec{v}_i,\ \frac{\mathrm{d}\vec{v}_i}{\mathrm{d}t}=\frac{\vec{f}_i}{m_i} \tag{1}$$

where $\vec{r}_i, \vec{v}_i, m_{i,}$ and $\vec{f}_i$ denote the position, velocity, mass of the *i* particle, and the force acting on it, respectively. The total force $\vec{f}_i$ acting on particle *i* is composed of conservative force F^{C}, random force F^{R}, and dissipative force F^{D}, each of which is pairwise interactions. The total force $\vec{f}_i$ is given by

$$\vec{f}_i=\sum_{j\neq i}\left(\vec{F}_{ij}^{\mathrm{C}}+\vec{F}_{ij}^{\mathrm{D}}+\vec{F}_{ij}^{\mathrm{R}}\right) \tag{2}$$

The sum of force acts over all particles within a certain cutoff radius r_{C}, beyond which the force is neglected.[4] Here r_{C} is the only length-scale in the system, which is considered as the unit of length, $r_{\mathrm{C}} = 1$. The conservation force of two particles is soft-repulsive interaction acting along the line of the centers of two particles:

$$\vec{F}_{ij}^{\mathrm{C}}=a_{ij}\omega\left(r_{ij}\right)\widehat{r}_{ij} \tag{3}$$

where a_{ij} is the interaction parameter between particles *i* and *j*. The *r*-dependent weight function $\omega(r_{ij})$ provides the range of interaction for DPD particles with a commonly used choice: $\omega\left(r_{ij}\right)=1-r_{ij}/r_{\mathrm{C}}$ for $r_{ij}\leq r_{\mathrm{C}}$ and $\omega\left(r_{ij}\right)=0$ for $r_{ij}> r_{\mathrm{C}}$. $\vec{r}_{ij}=\vec{r}_i-\vec{r}_j$, $r_{ij}=\left|\vec{r}_{ij}\right|$, and $\widehat{r}=\vec{r}_{ij}/r_{ij}$. The dissipative force which is proportional to the relative velocity, $\vec{v}_{ij}=\vec{v}_i-\vec{v}_j$, is defined as

$$\vec{F}_{ij}^{\mathrm{D}}=-\gamma\omega^{\mathrm{D}}\left(r_{ij}\right)\left(\widehat{r}_{ij}\bullet\vec{v}_{ij}\right)\widehat{r}_{ij} \tag{4}$$

where γ is the friction coefficient controlling the magnitude of the dissipative force. The random force acting as a heat source to equilibrate the thermal motion of unresolved scales is given by

$$\vec{F}_{ij}^{\mathrm{R}} = \sigma \omega^{\mathrm{R}}\left(r_{ij}\right)\theta_{ij}\hat{r}_{ij} \tag{5}$$

Where σ is the noise amplitude governing the intensity of the random force and $\theta_{ij}(t)$ is a randomly fluctuating variable with Gaussian statistics: $\left\langle \theta_{ij}(t) \right\rangle = 0$ and $\left\langle \theta_{ij}(t)\theta_{kl}(t') \right\rangle = \left(\delta_{ik}\delta_{jl} + \delta_{il}\delta_{jk}\right)\delta\left(t-t'\right)$.

Español and Warren[2] showed that the two weight functions $\omega^{\mathrm{D}}\left(r_{ij}\right)$ and $\omega^{\mathrm{R}}\left(r_{ij}\right)$ can be chosen arbitrarily and this choice fixes the other weight function, with the relation as shown in the following equation:

$$\omega^{\mathrm{D}}\left(r_{ij}\right) = \left[\omega^{\mathrm{R}}\left(r_{ij}\right)\right]^{2} \tag{6}$$

As a simple choice, we take $\omega^{\mathrm{R}}\left(r_{ij}\right) = \omega\left(r_{ij}\right)$, i.e., $\omega^{\mathrm{R}}\left(r_{ij}\right)$ is the same function as in the conservative force. There is also a relation between the two amplitudes and $k_{\mathrm{B}}T$:

$$\sigma^{2} = 2\gamma k_{\mathrm{B}}T\ . \tag{7}$$

The combined effect of the dissipative and random force amounts to that of a thermostat.

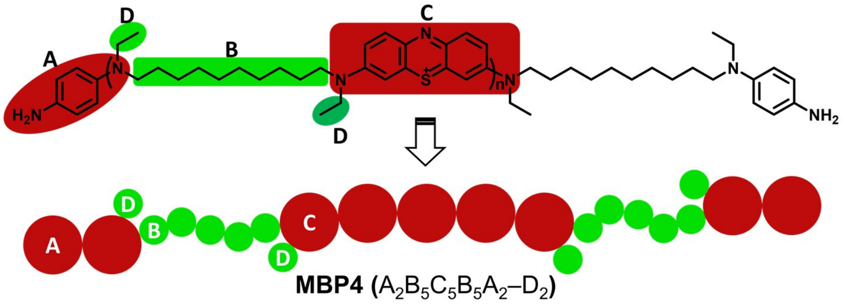

Fig. S1 The generic coarse–grained model of MBP4 (**$A_2B_5C_5B_5A_2$–D_1**).

The generic coarse-grained model (Fig. S1) was constructed based on MBP4 ($A_2B_5C_5B_5A_2$–D_2). There are four different types of DPD particles, A, B, C and D for end, middle alkyl chain (i.e., spacer), middle phenothiazinium group and side alkyl chain, respectively. “A” and “C” refers to a solvophobic block, “B” and “D” refers to a solvophilic block, and the subscript refers to the repeat units for corresponding blocks. The polymer will self–assemble in the co–solvent S1 and S2, where S1 is the good solvent for all the blocks and S2 is only good for blocks B and D. The concentration of polymer (ϕ_{P}) is defined as below:

$$\phi_{\mathrm{P}} = \frac{\mathrm{N_A V_A + N_B V_B + N_C V_C + N_D V_D}}{\mathrm{N_A V_A + N_B V_B + N_C V_C + N_D V_D + N_{S1} V_{S1} + N_{S2} V_{S2}}} \tag{1}$$

where N_A, N_B, N_C and N_S are the number of A bead, B bead, C bead and solvent bead in the simulation respectively, and V_A, V_B, V_C and V_S denote the volumes of the corresponding beads. The concentration of solvent (ϕ_S) is defined similarly.

All beads have the same size of r_c, except three beads of C represents benzene ring with the size of $1.2r_c$. And all the beads have the same mass as $m = 1$. Within MBP4, we use a finitely extensible nonlinear elastic (FENE) potential between the consecutive particles[5]: $V_{\mathrm{FENE}}(r_{ij}) = -1/2kR_0^2\ln[1-r_{ij}/R_0)^2]$ for $r_{ij} < R_0$ and $V_{\mathrm{FENE}}(r_{ij}) = \infty$ for $r_{ij} \geq R_0$. In our simulation, we set $k = 50$ and $R_0 = 1.5r_c$. To keep the anthryl group being rigid, a harmonic bending potential is also applied between beads C, which takes the form $U_\theta = 0.5k_\theta(\theta - \theta_0)^2$, where θ and θ_0 are the current and specified angles formed by the adjacent bonds and k_θ is a stiffness constant. Here, we set $k_\theta = 10$ and $\theta_0 = \pi$. The time scale is set to $(mr_c^2/\varepsilon)^{1/2}$, and the energy scale is given by $k_BT = 1$, where k_B is Boltzmann constant and T is the temperature. We use the modified Velocity-Verlet algorithm with $\lambda = 0.65$ in integrating the equation of motion. What's more, we set time step $\Delta t = 0.03$ and the amplitude of random noise $\sigma = 3.0$ to avoid divergence of the simulation.

For simplification, we set the number of middle repeated group BC $n = 1$. The copolymer MBP4 will self-assemble in the co-solvent S1 and S2, where S1 is the good solvent for all the blocks and S2 is only good for blocks B and D. The polymer concentration is set to be $\phi_p = 0.02$. The concentration of solvents is $\phi_{S1} = 0.48$, $\phi_{S2} = 0.50$. The length of spacer N_B and the side chain N_g can be varied. The interaction parameters chosen are shown in a symmetric matrix.

$$a_{ij} = \left\{ \begin{array}{ccccccc} & \mathrm{A} & \mathrm{B} & \mathrm{C} & \mathrm{D} & \mathrm{S1} & \mathrm{S2} \\ \mathrm{A} & 25 & & & & & \\ \mathrm{B} & 85 & 25 & & & & \\ \mathrm{C} & 25 & 85 & 25 & & & \\ \mathrm{D} & 85 & 25 & 85 & 25 & & \\ \mathrm{S1} & 25 & 25 & 25 & 25 & 25 & \\ \mathrm{S2} & 130 & 25 & 130 & 25 & 25 & 25 \end{array} \right\}$$

When we fix the three-dimension simulation with a fixed system number density of 3.0, the relationship between the a_{ij} and Flory-Huggins interaction parameters χ_{ij} is

$$a_{ij} \approx a_{ii} + 3.497\chi_{ij} . \tag{8}$$

We set $a_{ii} = 25$ for the same type of DPD particles (i = A, B, C, D), guaranteeing the correct excluded volume of the molecules. a_{ij} rises from 25 with increasing the incompatibility between particles i and j. Considering the relative position and chemical components of all the beads, we always keep $a_{\mathrm{AC}} = a_{\mathrm{BD}} = 25$, $a_{\mathrm{AB}} = a_{\mathrm{CD}} = 85$, $a_{\mathrm{AS1}} = a_{\mathrm{BS1}} = a_{\mathrm{CS1}} = a_{\mathrm{DS1}} = 25$, $a_{\mathrm{AS2}} = a_{\mathrm{CS2}} = 130$, and $a_{\mathrm{BS2}} = a_{\mathrm{DS2}} = 25$. We perform the dynamics of total 81 000 DPD beads in a cubic box (30^3) under the periodic boundary conditions. In these conditions, we carry out 2.0×10^6 steps for each simulation.

Supplementary figures

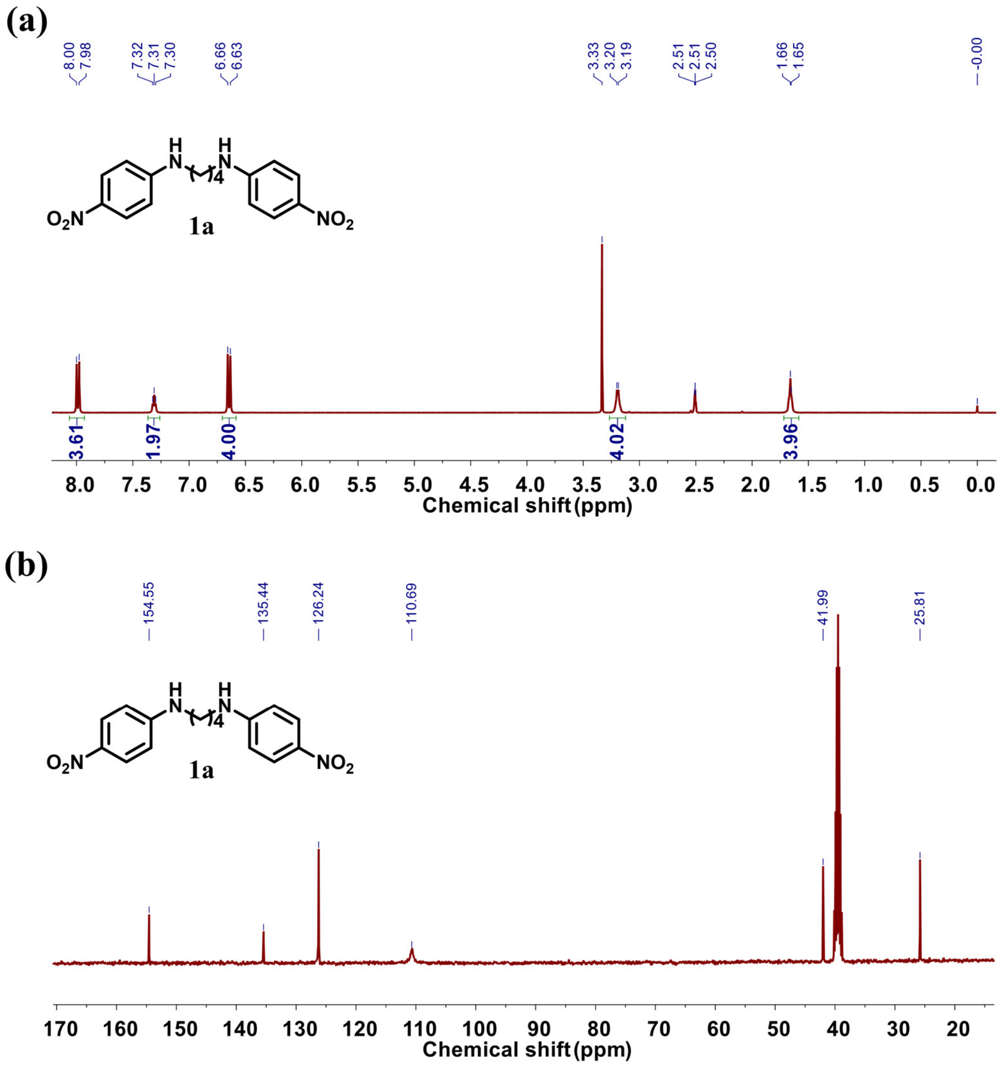

Fig. S2 The ^{1}H NMR spectrum (a) and ^{13}C NMR spectrum (b) of **1a** in DMSO–d6.

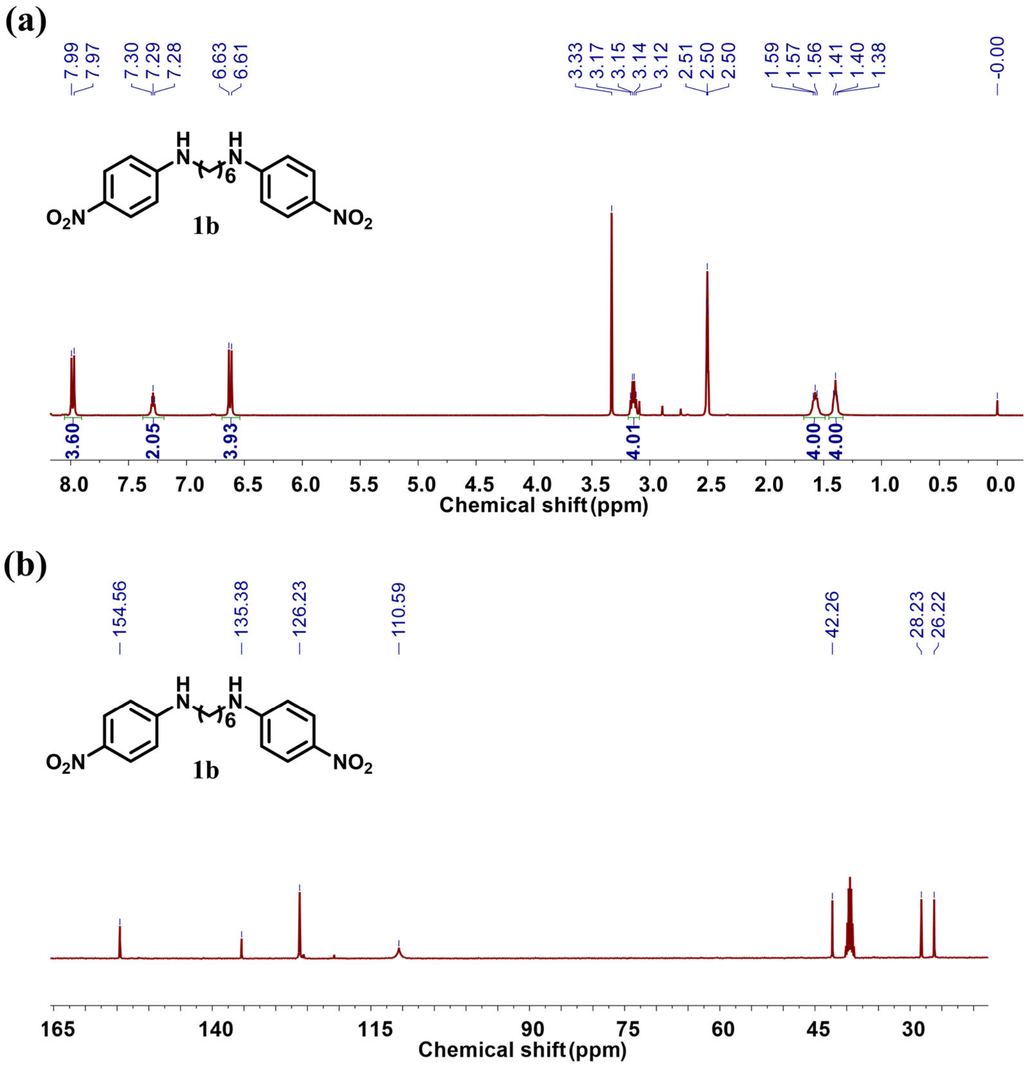

Fig. S3 The ^{1}H NMR spectrum (a) and ^{13}C NMR spectrum (b) of **1b** in DMSO–d6.

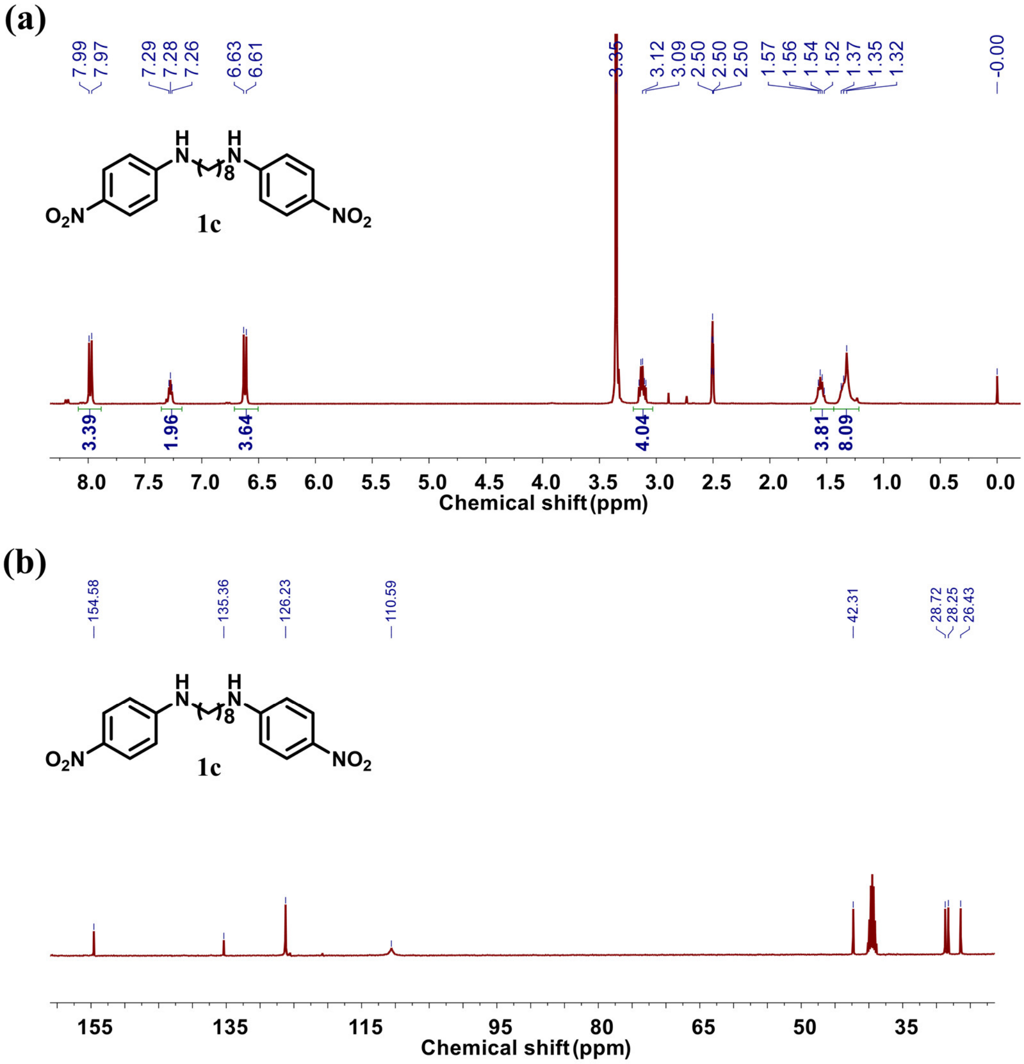

Fig. S4 The ^{1}H NMR spectrum (a) and ^{13}C NMR spectrum (b) of **1c** in DMSO–d6.

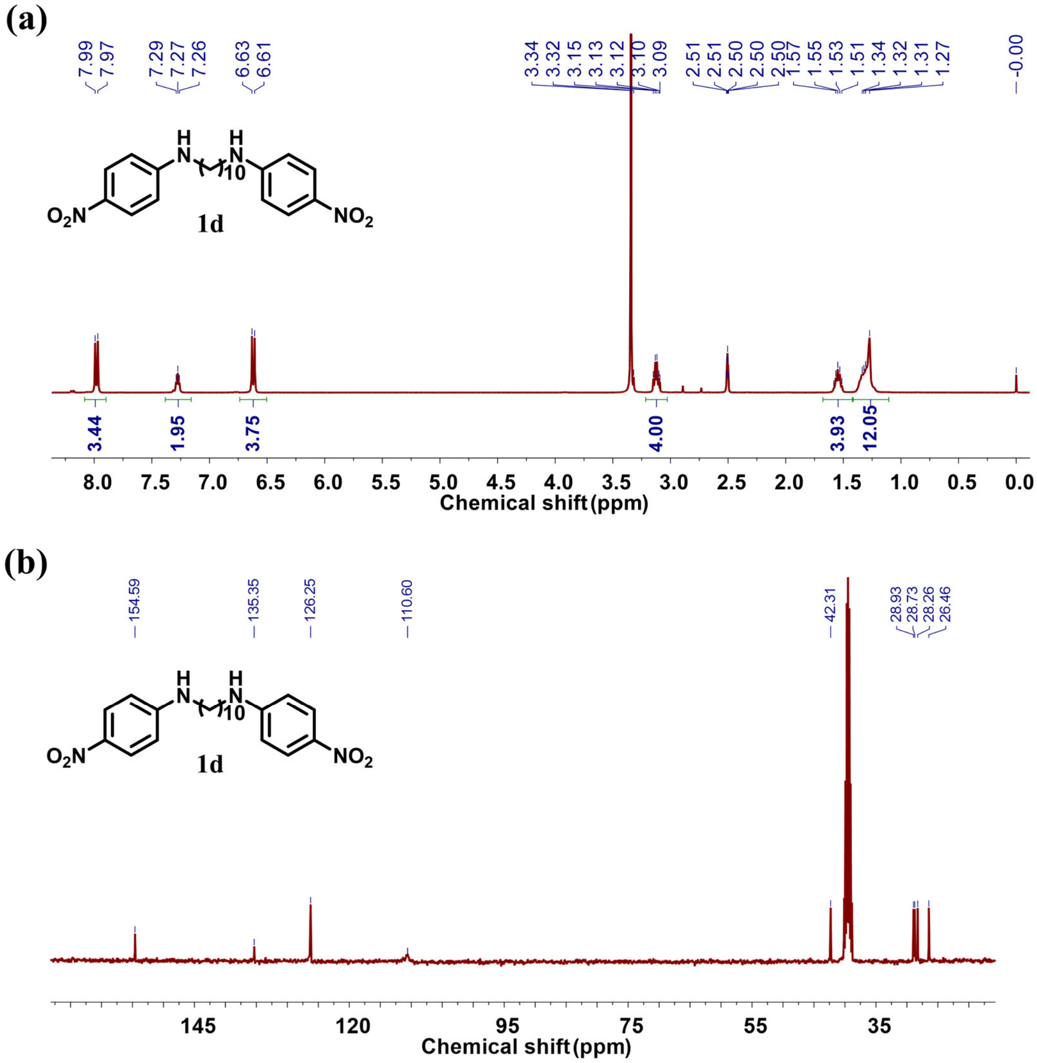

Fig. S5 The ^{1}H NMR spectrum (a) and ^{13}C NMR spectrum (b) of **1d** in DMSO–d6.

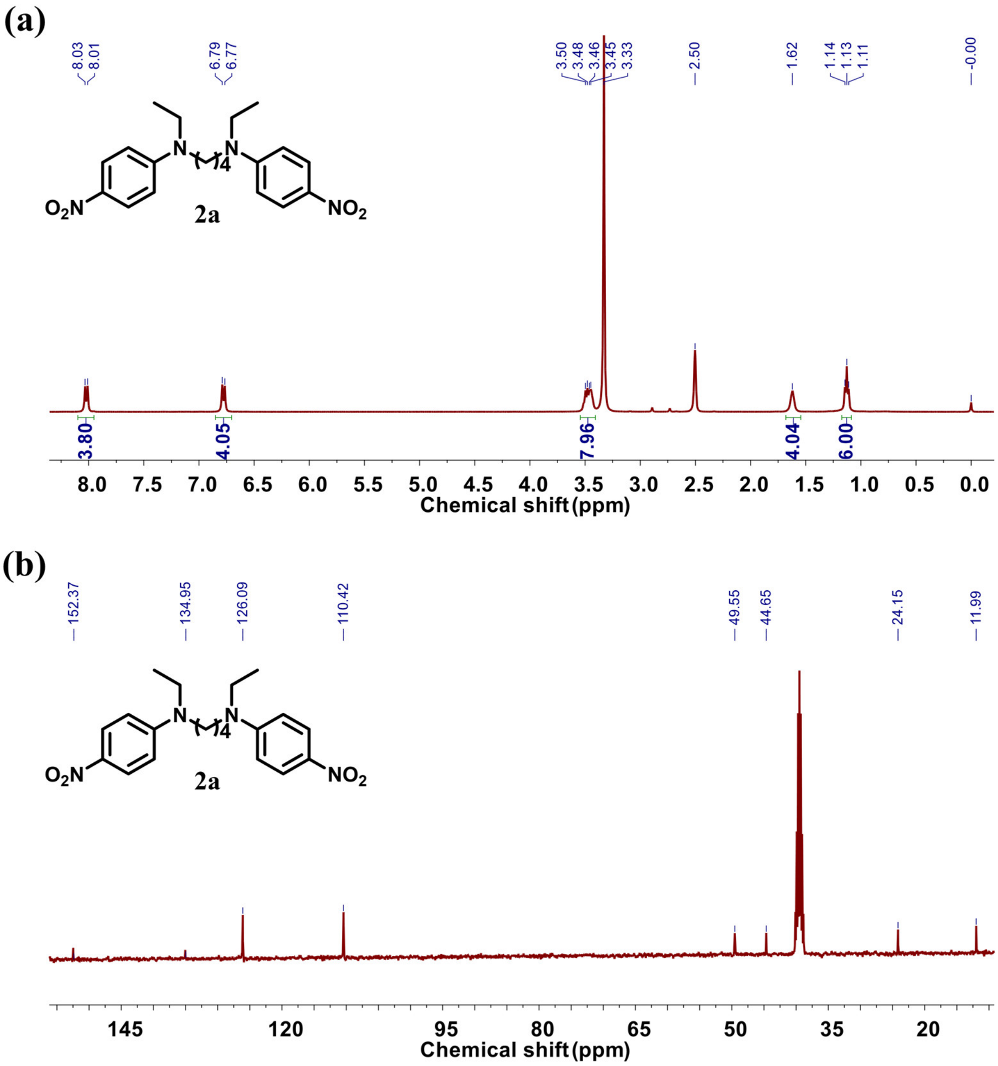

Fig. S6 The ^{1}H NMR spectrum (a) and ^{13}C NMR spectrum (b) of **2a** in DMSO–d6.

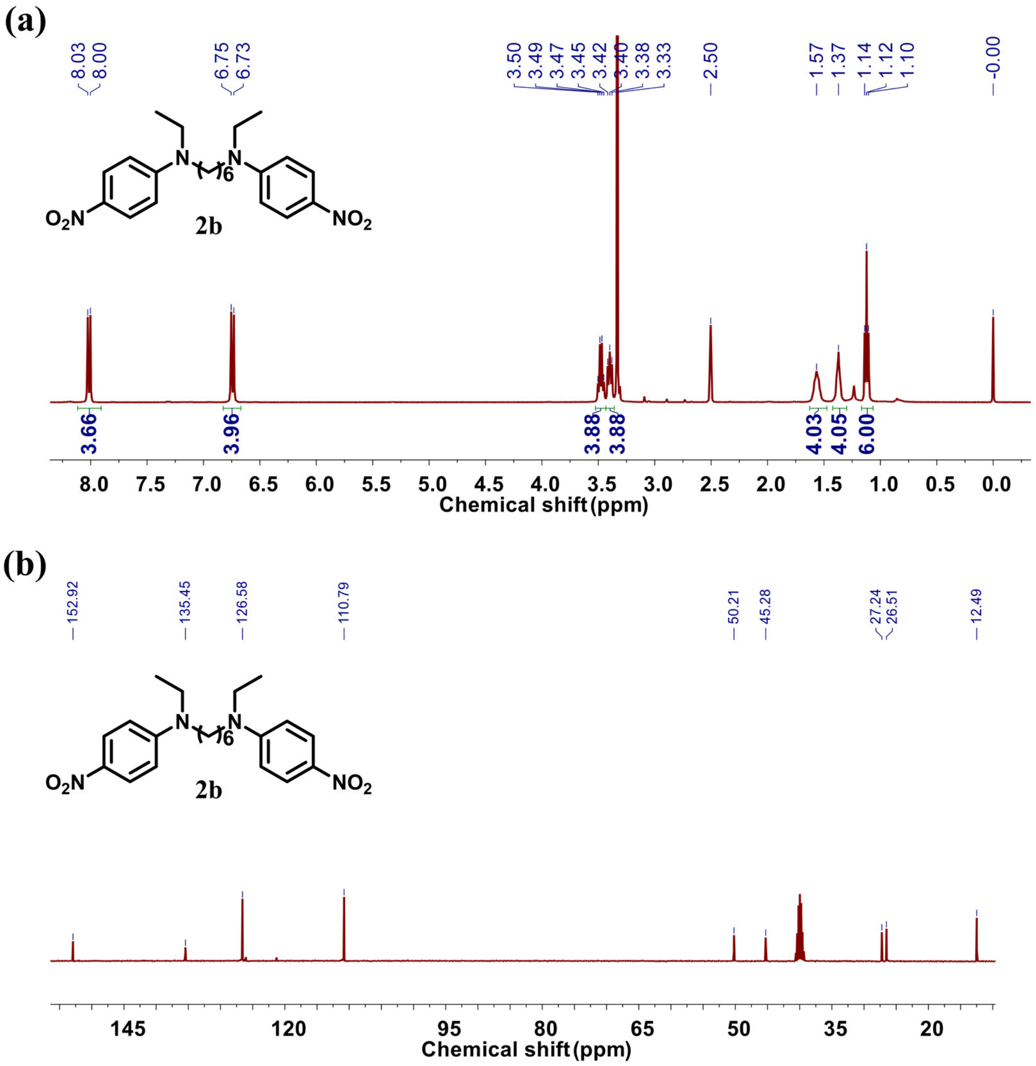

Fig. S7 The ^{1}H NMR spectrum (a) and ^{13}C NMR spectrum (b) of **2b** in DMSO–d6.

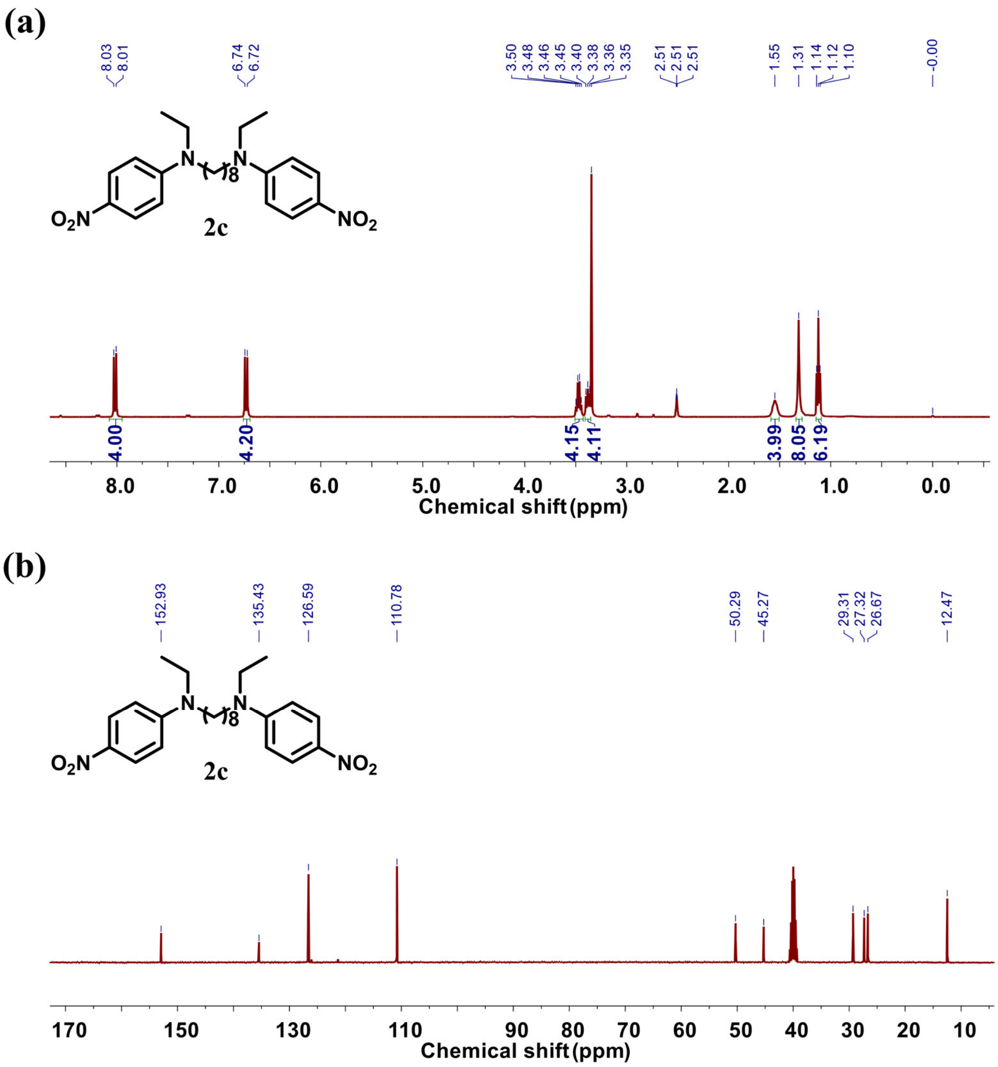

Fig. S8 The ^{1}H NMR spectrum (a) and ^{13}C NMR spectrum (b) of **2c** in DMSO–d6.

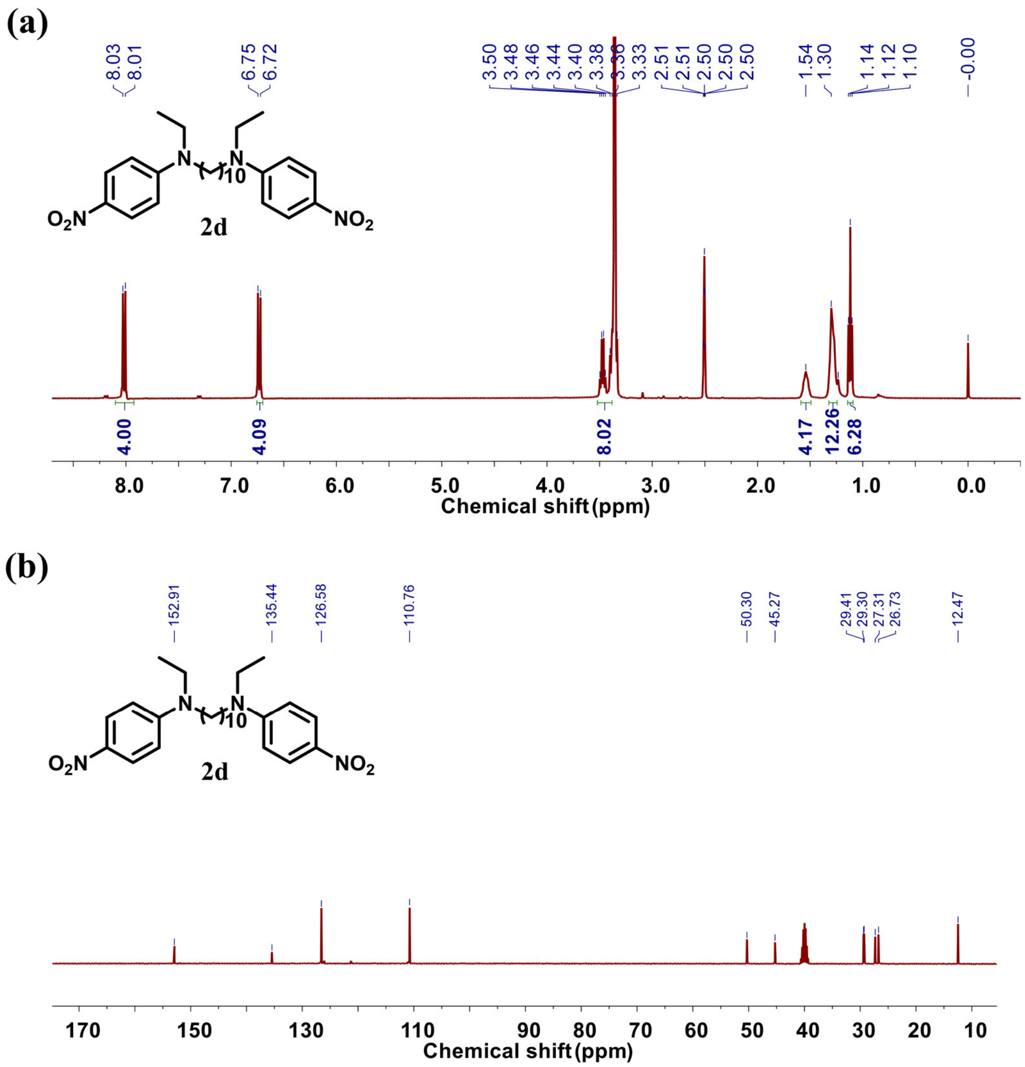

Fig. S9 The ^{1}H NMR spectrum (a) and ^{13}C NMR spectrum (b) of **2d** in DMSO–d6.

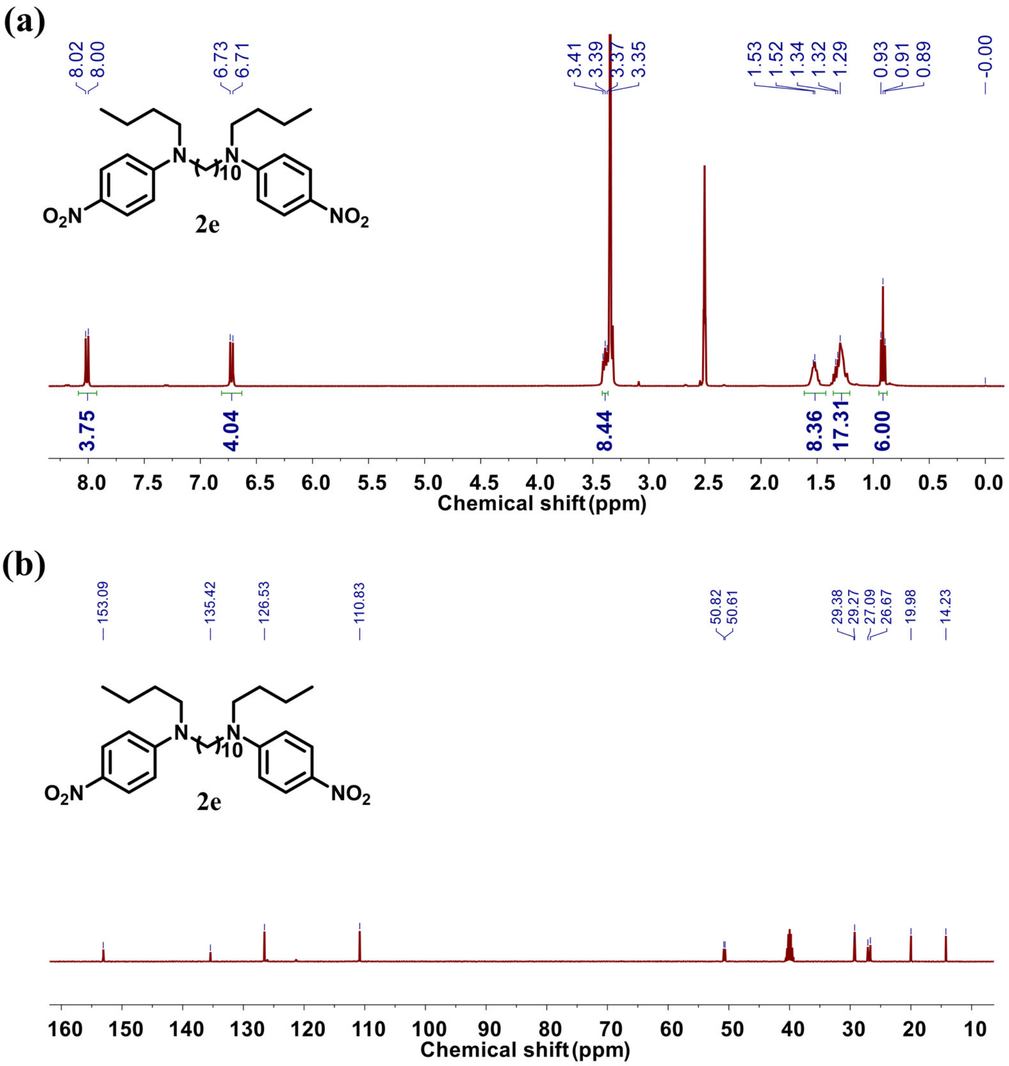

Fig. S10 The ^{1}H NMR spectrum (a) and ^{13}C NMR spectrum (b) of **2e** in DMSO–d6.

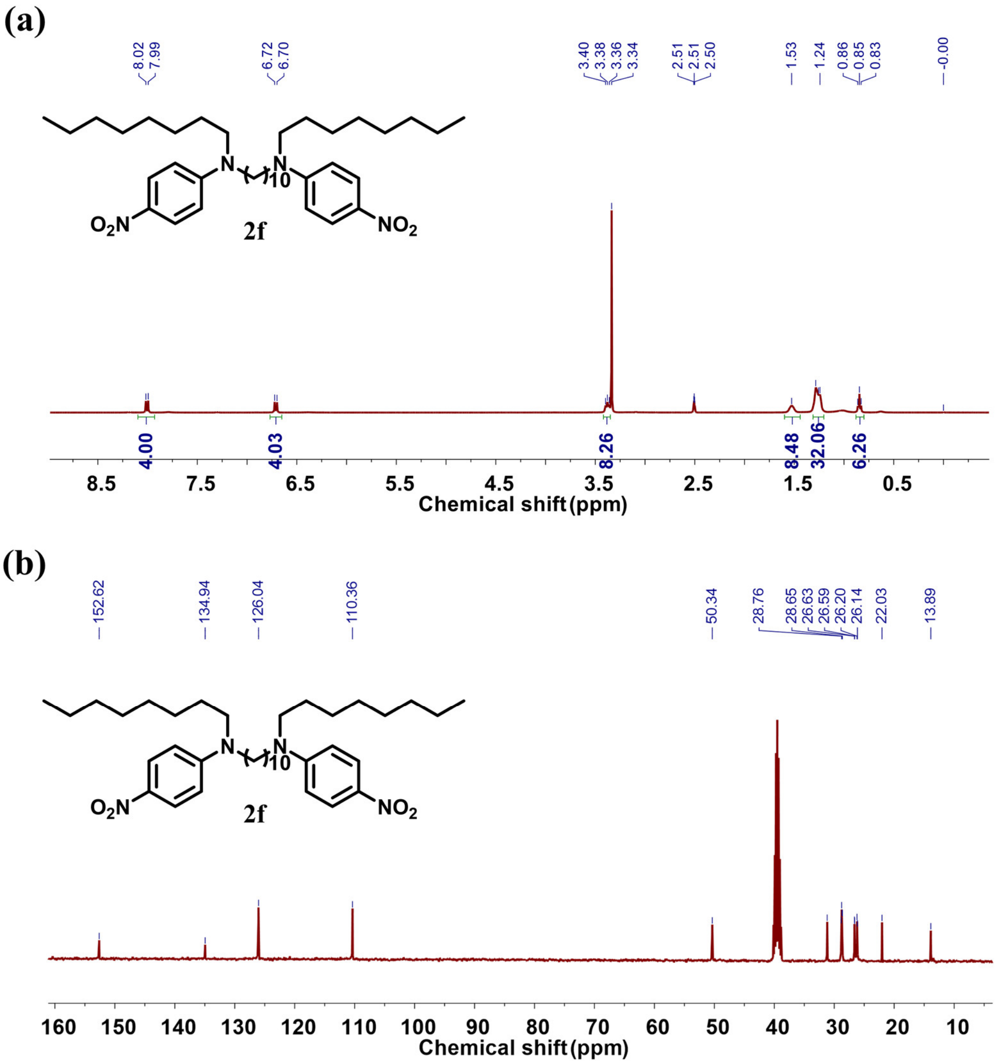

Fig. S11 The ^{1}H NMR spectrum (a) and ^{13}C NMR spectrum (b) of **2f** in DMSO–d6.

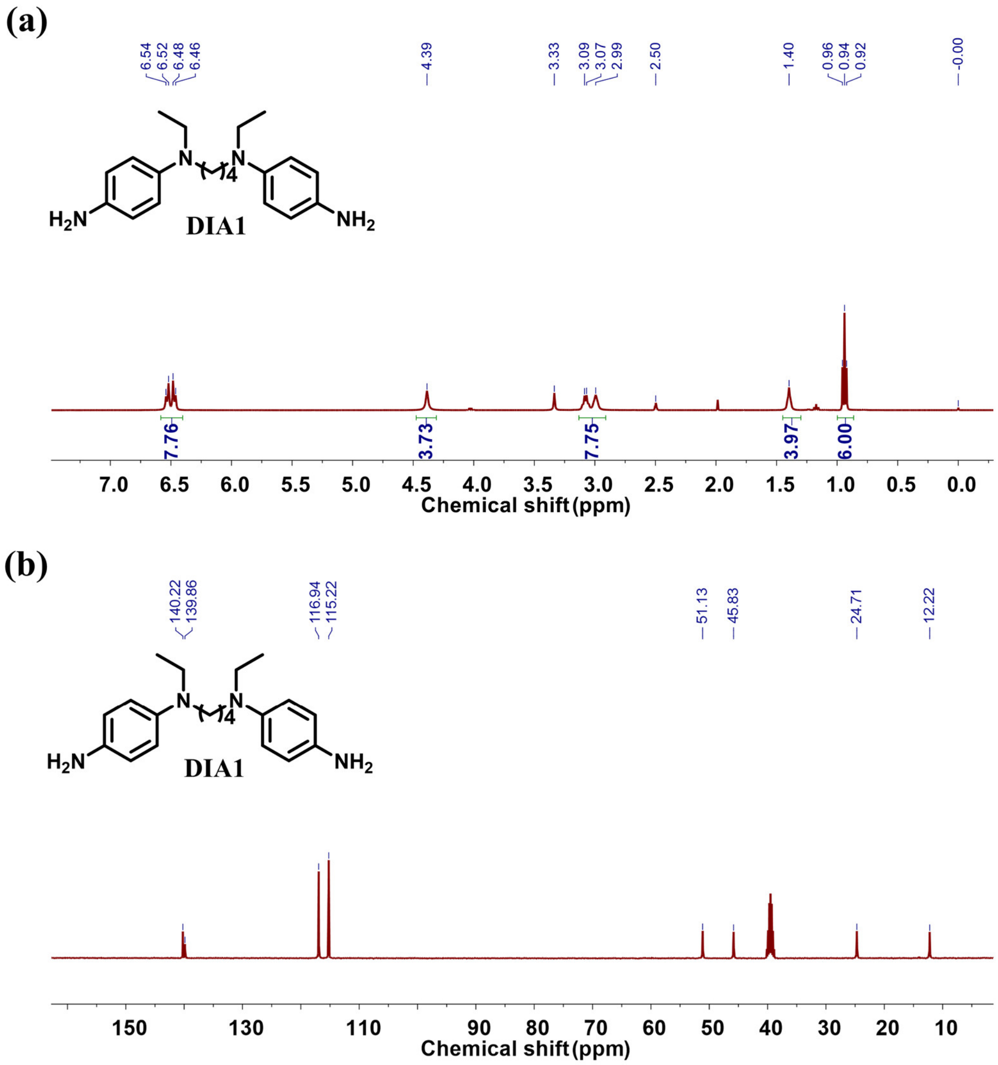

Fig. S12 The ^{1}H NMR spectrum (a) and ^{13}C NMR spectrum (b) of DIA1 in DMSO–d6.

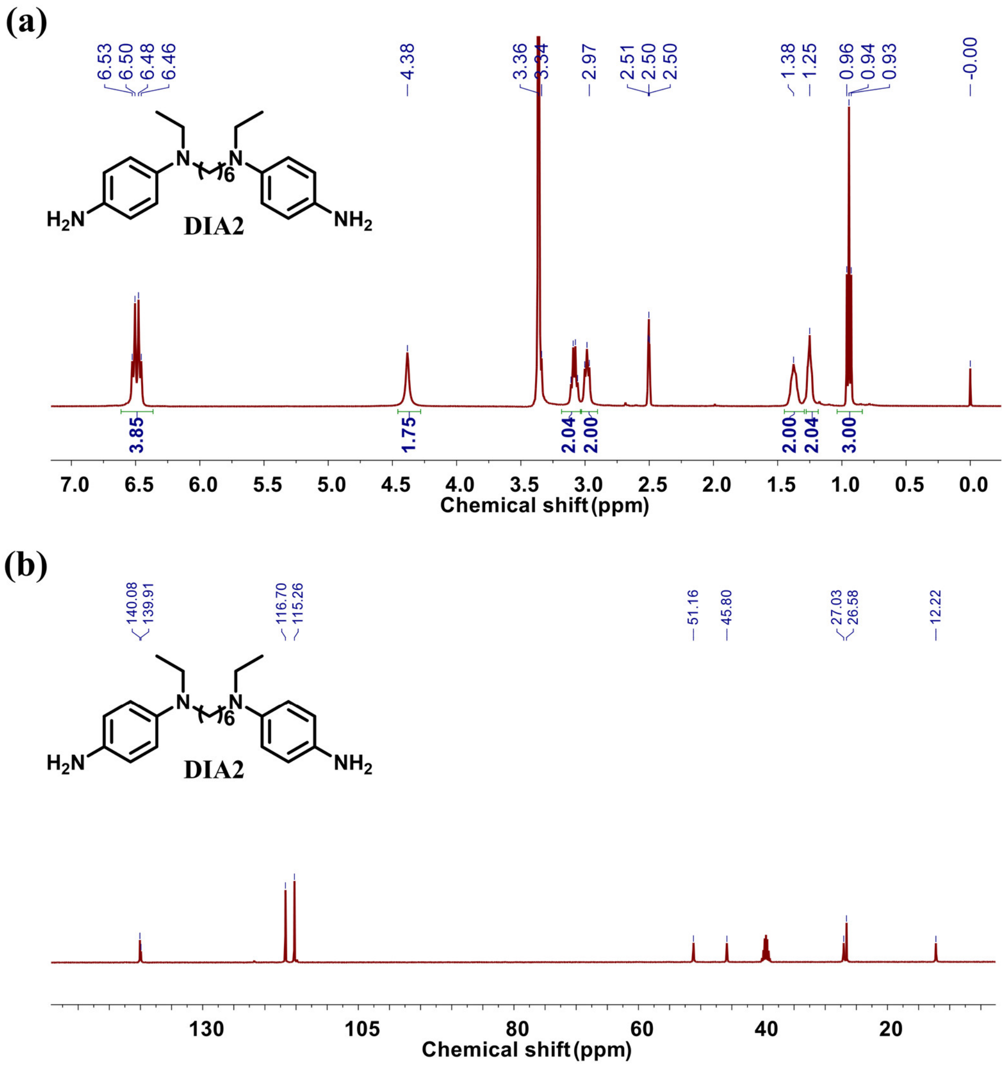

Fig. S13 The ^{1}H NMR spectrum (a) and ^{13}C NMR spectrum (b) of DIA2 in DMSO–d6.

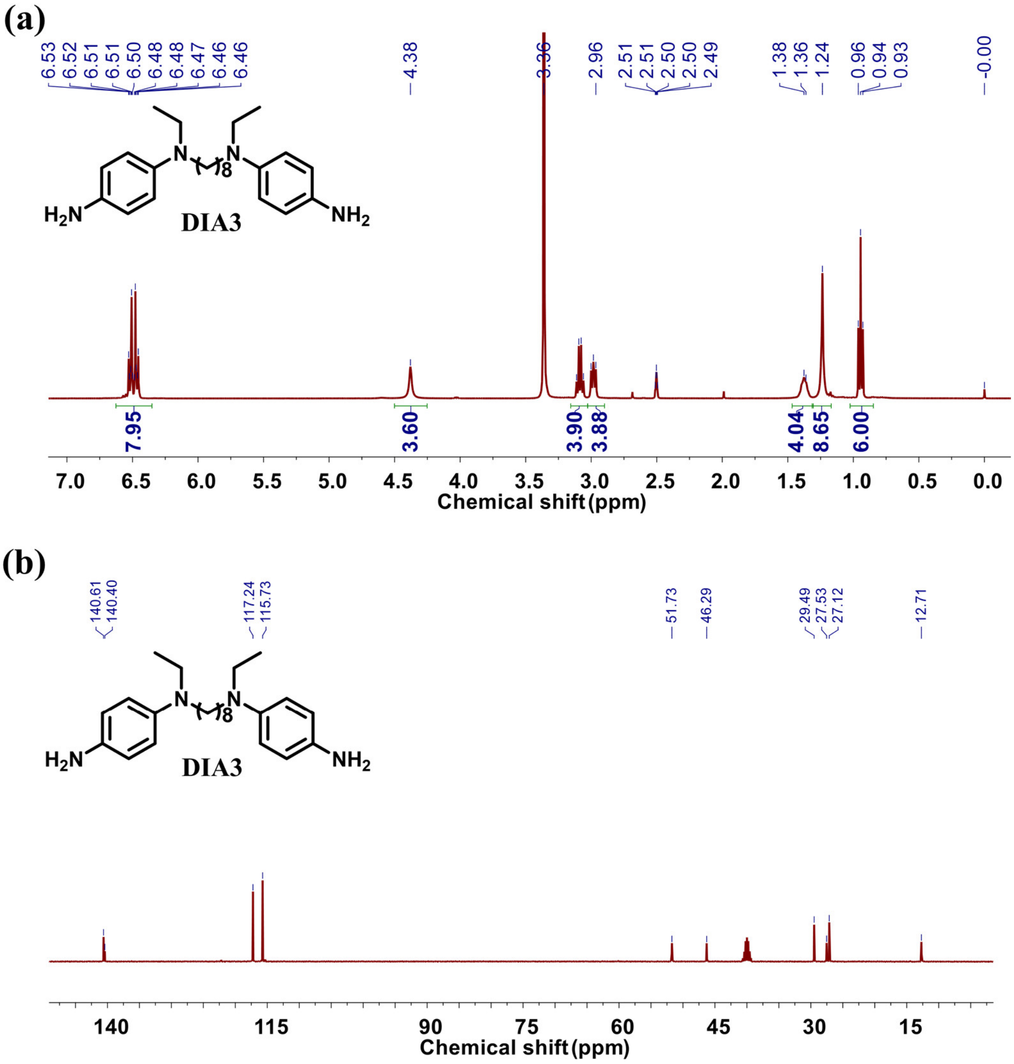

Fig. S14 The ^{1}H NMR spectrum (a) and ^{13}C NMR spectrum (b) of DIA3 in DMSO–d6.

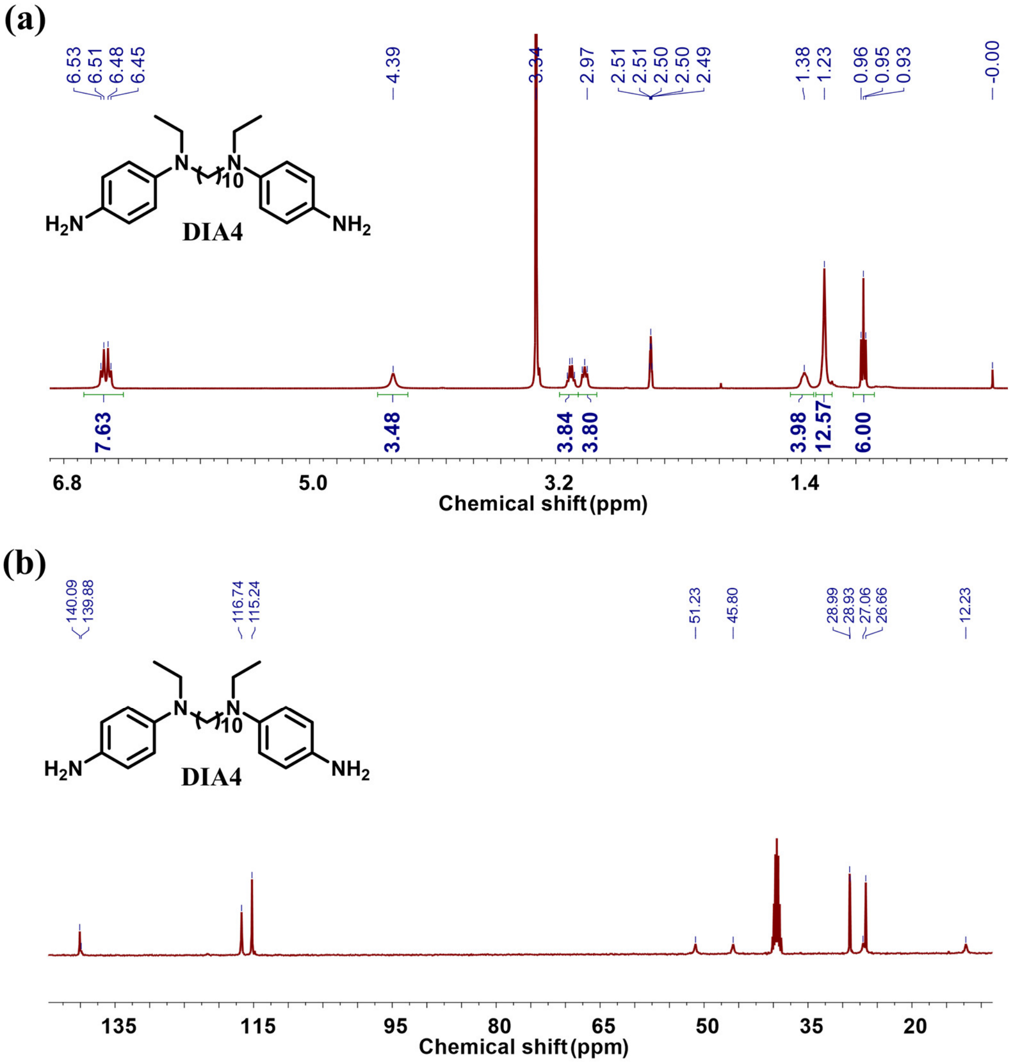

Fig. S15 The ^{1}H NMR spectrum (a) and ^{13}C NMR spectrum (b) of DIA4 in DMSO–d6.

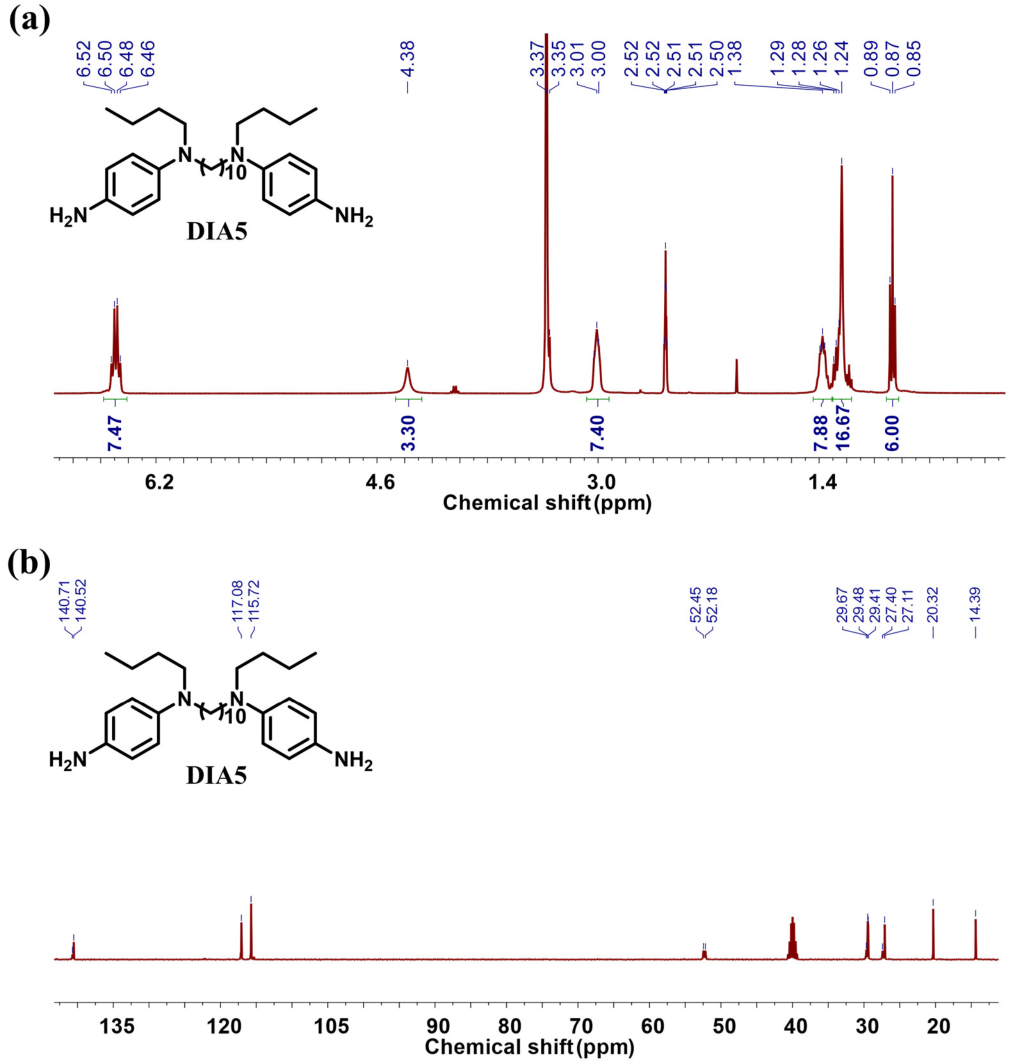

Fig. S16 The ^{1}H NMR spectrum (a) and ^{13}C NMR spectrum (b) of DIA5 in DMSO–d6.

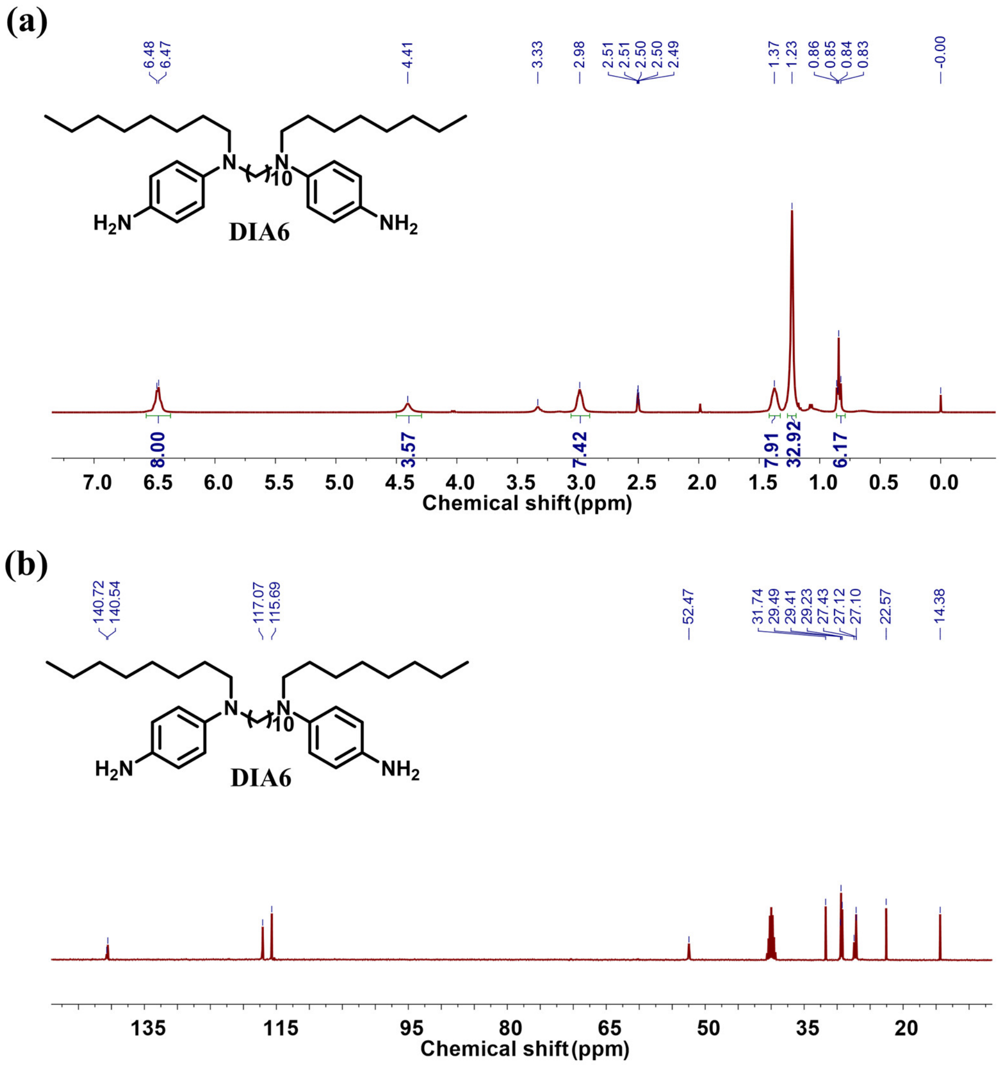

Fig. S17 The ^{1}H NMR spectrum (a) and ^{13}C NMR spectrum (b) of DIA6 in DMSO–d6.

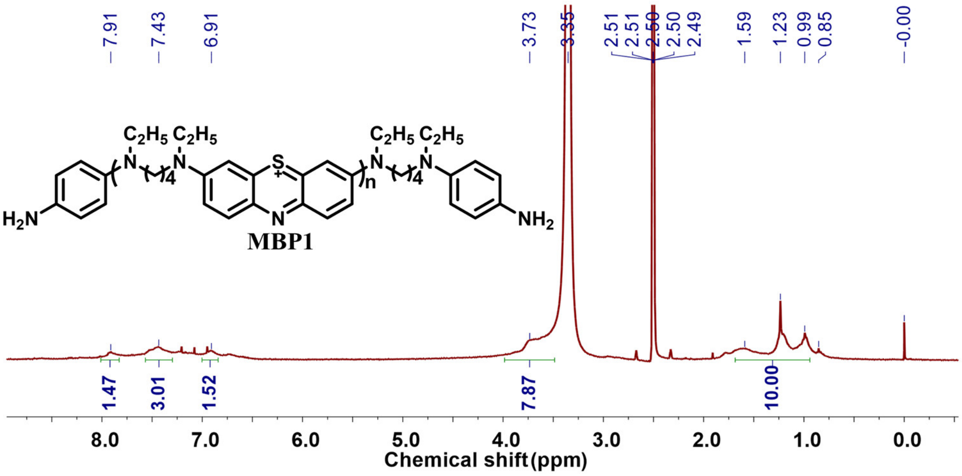

Fig. S18 The ^{1}H NMR spectrum of MBP1 in DMSO–d6.

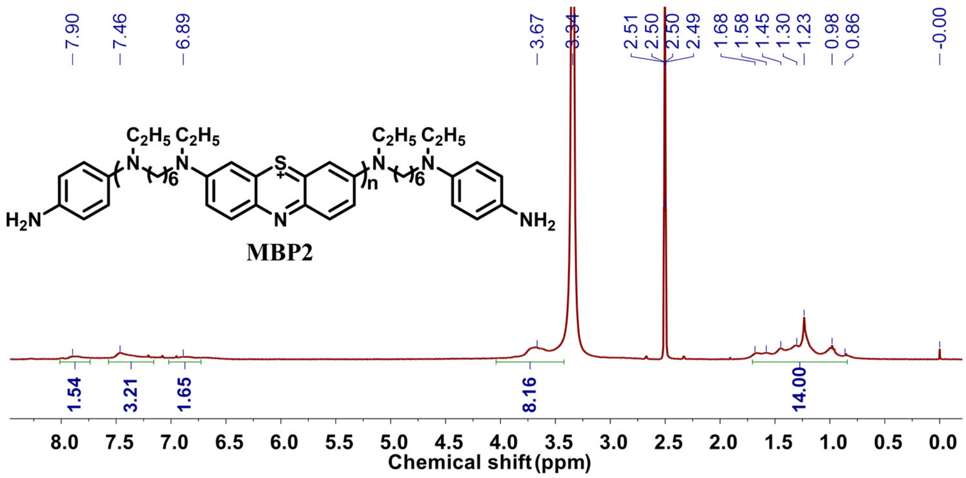

Fig. S19 The ^{1}H NMR spectrum of MBP2 in DMSO–d6.

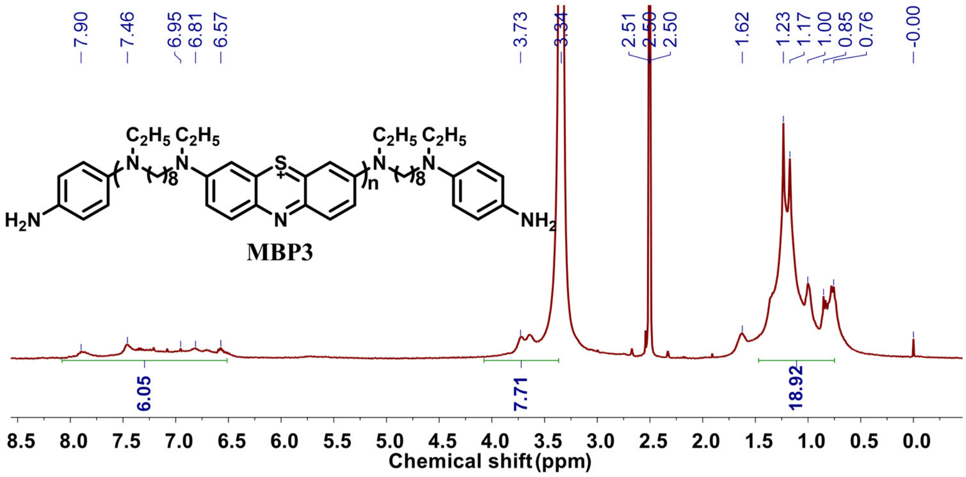

Fig. S20 The ^{1}H NMR spectrum of MBP3 in DMSO–d6.

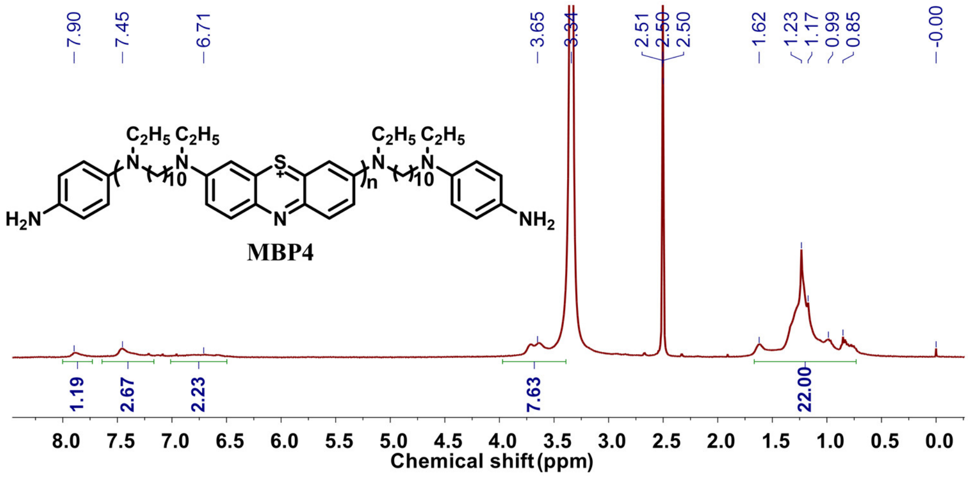

Fig. S21 The ^{1}H NMR spectrum of MBP4 in DMSO–d6.

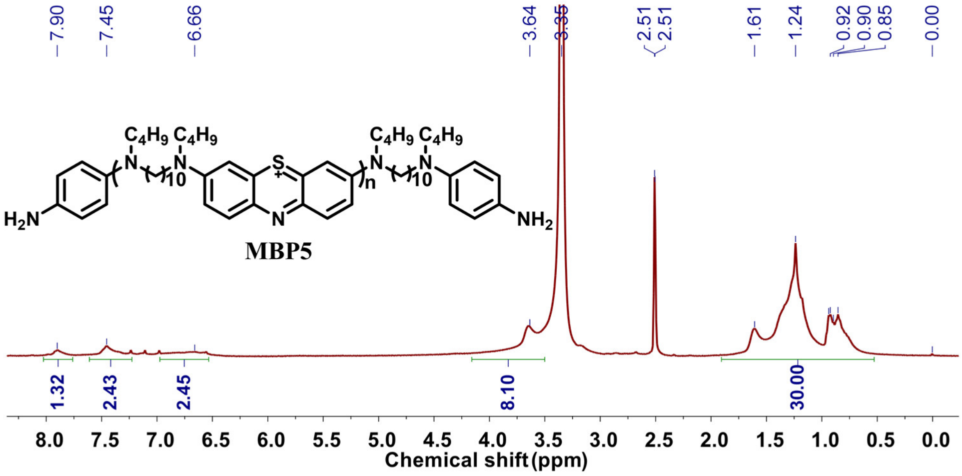

Fig. S22 The ^{1}H NMR spectrum of MBP5 in DMSO–d6.

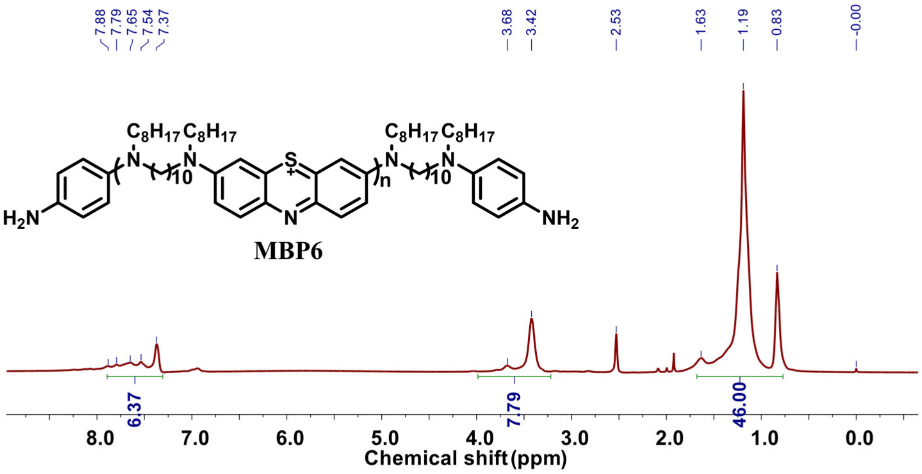

Fig. S23 The ^{1}H NMR spectrum of MBP6 in DMSO–d6.

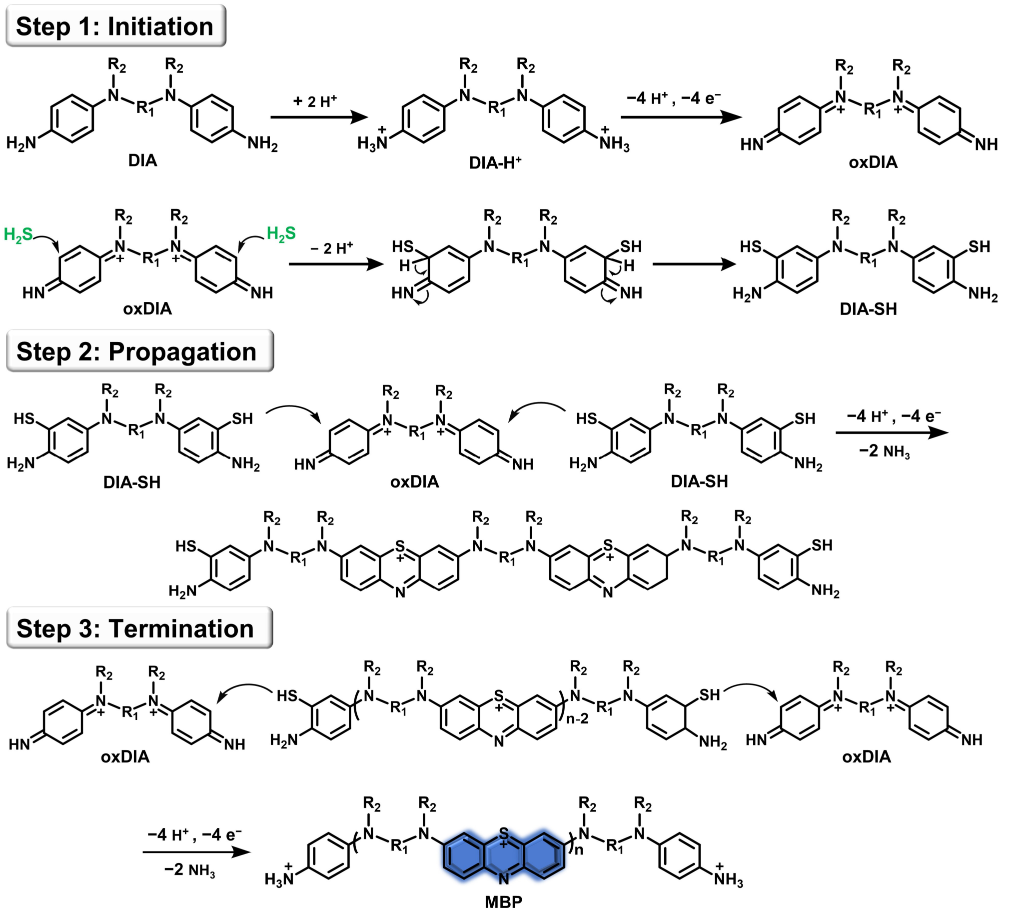

Fig. S24 Proposed mechanism of MBP polymerization. R_1 and R_2 represent $R_{N\text{-}sp}$ and $R_{N\text{-}sc}$, respectively.

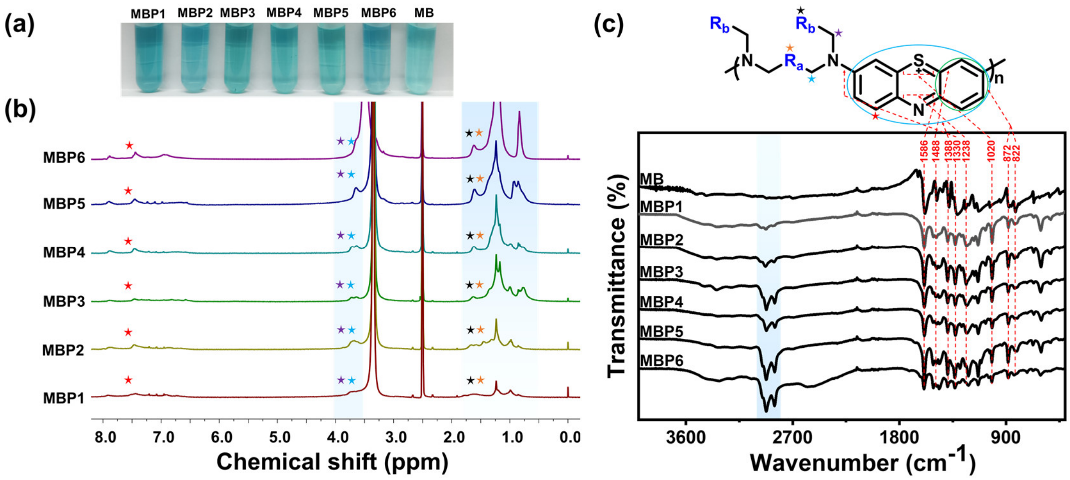

Fig. S25 (a) Photographs of MBPs and MB in DMSO. (b) ^{1}H NMR spectra of MBPs in deuterated DMSO. (c) FT-IR spectra of MBPs and MB.

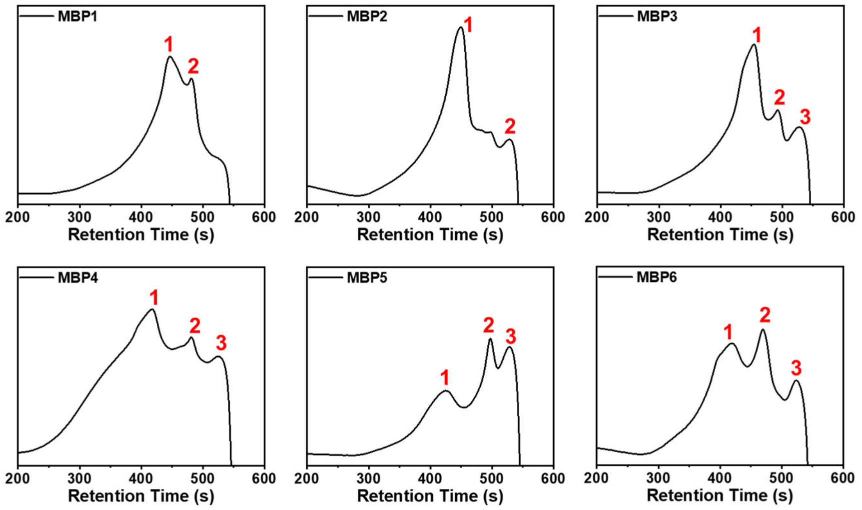

Fig. S26 GPC traces of MBPs in DMF.

Table S1 GPC data of MBPs.

Polymer	**Peak**[a]	M_n[b]	M_w[b]	$Đ$
MBP1	1	125 kDa	138 kDa	1.10
	2	48.1 kDa	48.4 kDa	1.01
MBP2	1	128 kDa	139 kDa	1.08
	2	15.9 kDa	15.9 kDa	1.00
MBP3	1	119 kDa	129 kDa	1.09
	2	38.3 kDa	38.9 kDa	1.02
	3	16.2 kDa	16.5 kDa	1.02
MBP4	1	301 kDa	337 kDa	1.12
	2	54.2 kDa	57.1 kDa	1.05
	3	16.0 kDa	16.4 kDa	1.03
MBP5	1	216 kDa	237 kDa	1.09
	2	34.7 kDa	35.2 kDa	1.01
	3	15.7 kDa	15.9 kDa	1.01
MBP6	1	309 kDa	368 kDa	1.19
	2	66.9 kDa	69.8 kDa	1.04
	3	15.8 kDa	16.2 kDa	1.03

[a] The number of GPC peak as indicated in Fig. S26. [b] Measured by GPC using polystyrene as a standard in DMF.

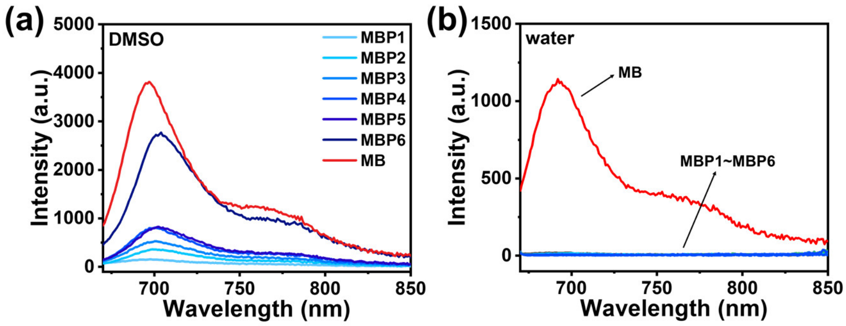

Fig. S27 (a) Fluorescence spectra of MBPs and MB in DMSO. (b) Fluorescence spectra of MBPs and MB in water.

Table S2 Absorption wavelength corresponding to A_1 and A_2 in DMSO and water.

Solvent	Type	MBP1	MBP2	MBP3	MBP4	MBP5	MBP6	MB
DMSO	A_1^a	628 nm	630 nm	631 nm	631 nm	631 nm	633 nm	621 nm
	A_2^b	674 nm	678 nm	676 nm	676 nm	678nm	679 nm	670 nm
Water	A_1^c	628 nm	628 nm	629 nm	626 nm	628 nm	629 nm	612 nm
	A_2^d	670 nm	675 nm	676 nm	671 nm	672nm	674 nm	664 nm

[a] The intensity of absorption band characteristic for aggregated MB in DMSO.

[b] The intensity of absorption band characteristic for monomeric MB in DMSO.

[c] The intensity of absorption band characteristic for aggregated MB in water.

[d] The intensity of absorption band characteristic for monomeric MB in water.

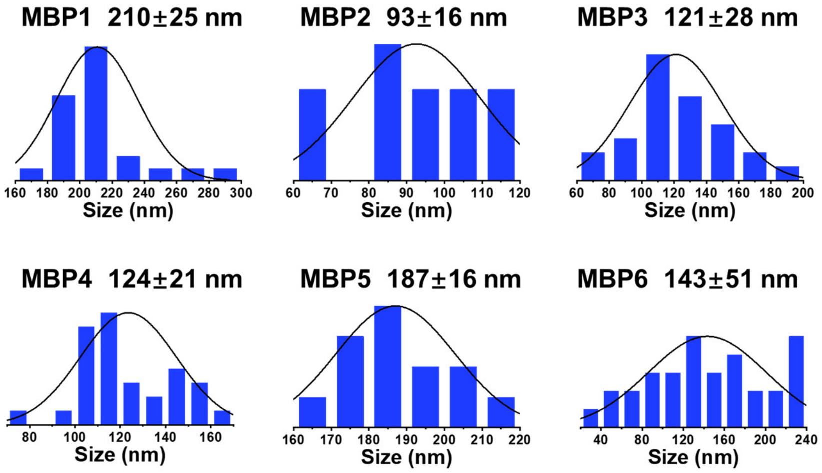

Fig. S28 The size histograms from TEM images of MBPs nano-assemblies.

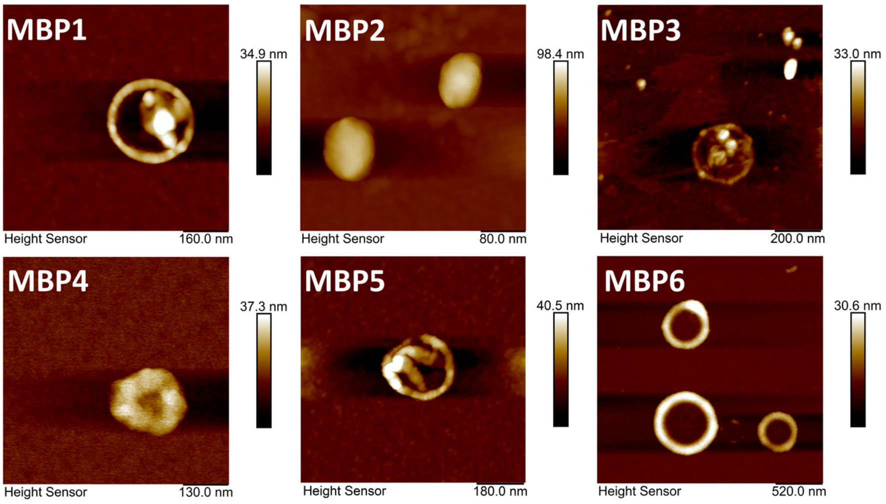

Fig. S29 AFM images of MBPs prepared at a concentration of 0.2 mg mL^{-1} in THF/DMSO (1:1, v/v).

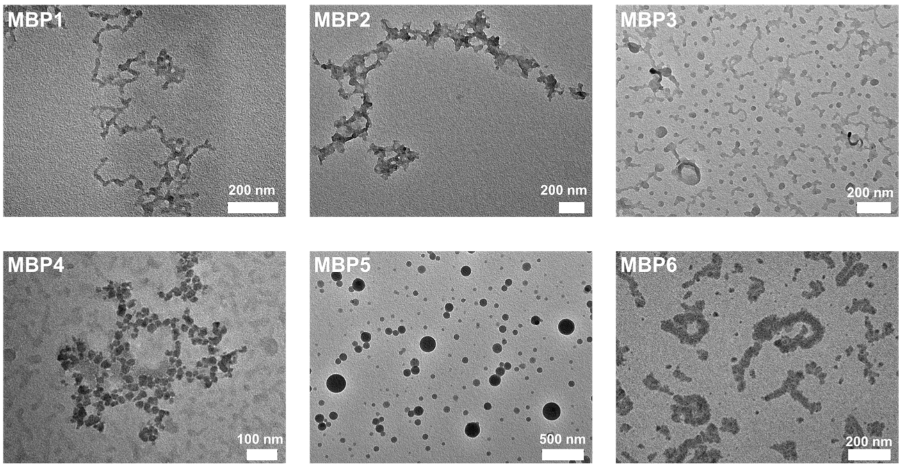

Fig. S30 TEM images of MBPs prepared at a concentration of 0.2 mg mL^{-1} in water/DMSO (9:1, v/v).

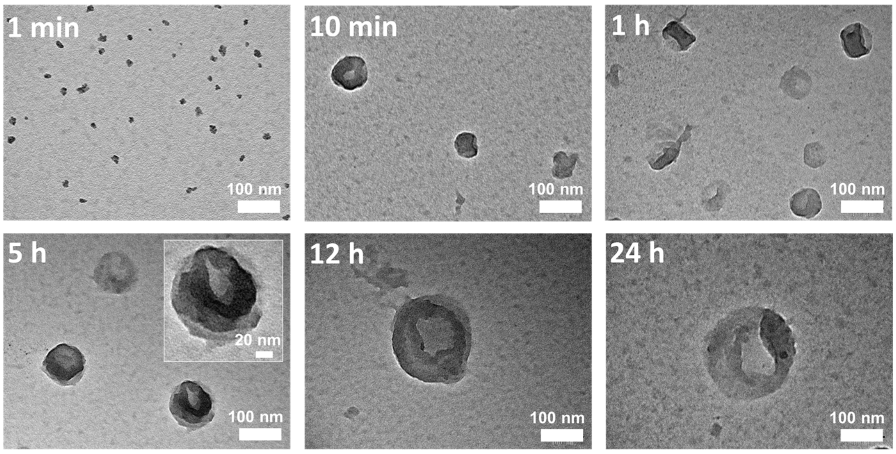

Fig. S31 TEM images of MBP1 prepared at a concentration of 0.2 mg mL^{-1} in THF/DMSO (1:1, v/v) for various periods.

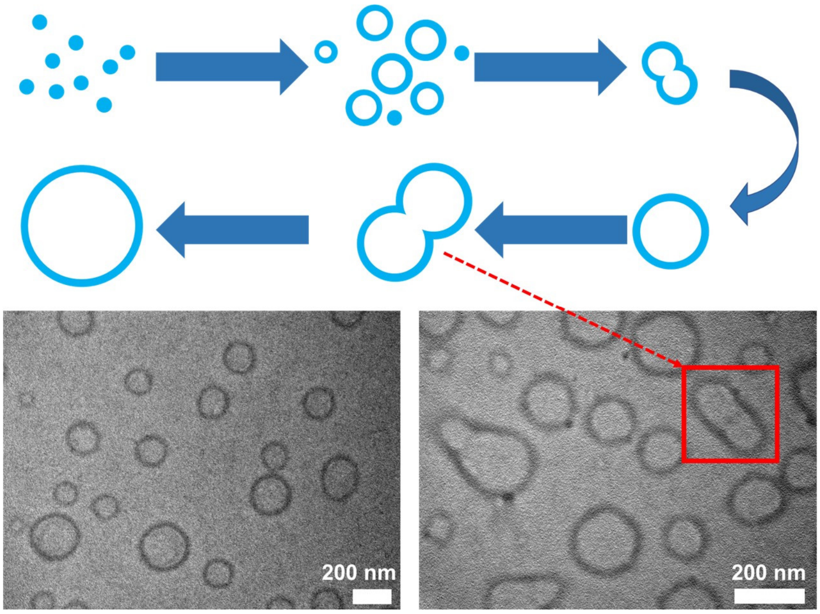

Fig. S32 Schematic diagram of nanoring formation.

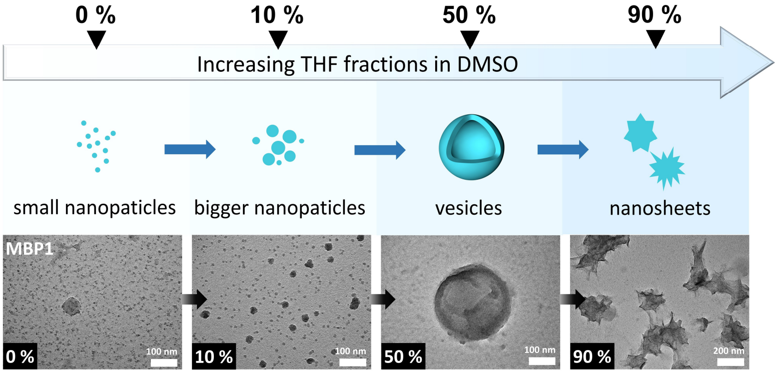

Fig. S33 Top: Schematic diagram of MBP1 self-assembly upon increasing the THF fraction in DMSO. Bottom: TEM images of MBP1 prepared at a concentration of 0.2 mg mL^{-1} in DMSO containing 0−90 v % THF.

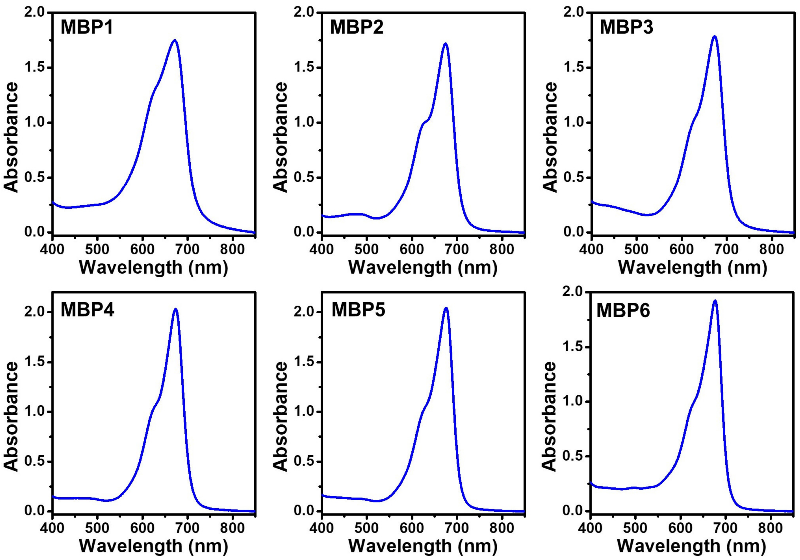

Fig. S34 The UV/Vis absorption spectra of MBP solutions that were prepared at a concentration of 0.2 mg mL^{-1} in THF/DMSO (1: 1, v/v).

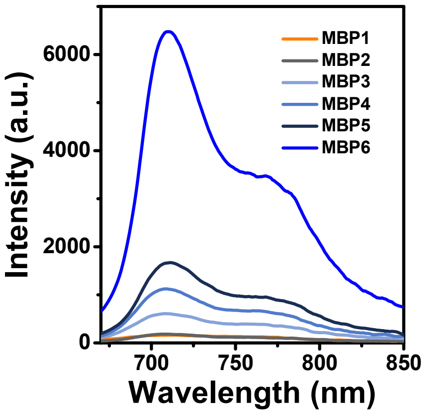

Fig. S35 Fluorescence spectra of MBPs solutions that were prepared at a concentration of 0.2 mg mL^{-1} in THF/DMSO (1: 1, v/v).

Table S3 Spectroscopic properties of MBPs in THF/DMSO (1: 1, v/v).

Polymer	**MBP1**	**MBP2**	**MBP3**	**MBP4**	**MBP5**	**MBP6**
λ_{A1}(nm)[a]	626	629	630	629	630	631
λ_{A2}(nm)[b]	671	674	673	673	675	676
A_1/A_2	0.74	0.59	0.59	0.53	0.52	0.51
λ_{em}(nm)[c]	710	707	708	708	711	709

[a] The absorption wavelength corresponding to A_1.

[b] The absorption wavelength corresponding to A_2.

[c] The maximum fluorescence emission wavelength of MBPs with excitation at 660 nm.

References

1 P. J. Hoogerbrugge, J. Koelman, *Europhys. Lett.*, 1992, **19**, 155-160.

2 P. Espanol, P. Warren, *Europhys. Lett.*, 1995, **30**, 191-196.

3 X. Liu, K. Yang, H. Guo, *J. Phys. Chem. B*, 2013, **117**, 9106-9120.

4 R. D. Groot, P. B. Warren, *J. Chem. Phys.*, 1997, **107**, 4423-4435.

5 M. Kroger, S. Hess, *Phys. Rev. Lett.*, 2000, **85**, 1128-1131.